This is to certify that the

thesis entitled

Determining Stereochemical Relationships:
Synthesis of Poly(lactide) Hexads

presented by

Erin E. Paske

has been accepted towards fulfillment
of the requirements for

M.S. degree in Chemistry

Major professor

Date May 8, 2002

DETERMINING STEREOCHEMICAL RELATIONSHIPS: SYNTHESIS OF POLY(LACTIDE) HEXADS

By

Erin E. Paske

A Thesis

Submitted to

Michigan State University

In partial fulfillment of the requirements

for the degree of

MASTER OF SCIENCE

Department of Chemistry

2002

ABSTRACT

DETERMINING STEREOCHEMICAL RELATIONSHIPS: SYNTHESIS OF POLY(LACTIDE) HEXADS

By

Erin E. Paske

The polylactides are environmentally benign polymers with applications as biodegradable and bioresorbable materials. The physical properties of polylactides depend on the crystallinity of the polymer, which in turn are determined by the regularity of the distribution of stereocenters in the backbone of the polylactide chain. A powerful tool for determining the regularity of polymers is the use of Nuclear Magnetic Resonance (NMR) in conjunction with well-defined model compounds and modeling. To date, interpretations of the NMR spectrum of polylactide have often been contradictory.

Poly(lactide) hexads of known stereochemistry were synthesized using an iterative procedure and characterized by NMR to firmly establish the NMR assignments. Comparisons of the ^{13}C NMR spectra of various hexads and shorter oligomers allowed assignment of the methine region of the spectra. A simple additivity model that considers the effects of neighboring and next-nearest neighboring stereocenters provides reasonable agreement with the experimental results.

ACKNOWLEDGMENTS

Several people have made my time at Michigan State University a pleasant experience. I would like to thank Dr. Baker for his guidance and support through grad school. Without the NMR help of Kermit Johnson, Long Lee, and Art Bates, much of this work would have not been possible.

Current and former Baker group members have made being a grad student a fun experience. My gratitude goes out to Cory, Micah, J. B., Tianqi, Chun, Tara, Kirk, Mao, Gao, Bao, Ping, Ying, Xuwei, Fung, Leslie, Nate, and Gia. Lunches were made even better by Leslie, Nate, and Kirk.

I would also like to thank my family and other friends who supported me through grad school. Thanks for listening and being there when I needed you.

TABLE OF CONTENTS

LIST OF TABLES

LIST OF FIGURES

LIST OF SCHEMES

ABBREVIATIONS

COSY	Correlated Spectroscopy
DCC	Dicyclohexylcarbodiimide
DCU	Dicyclohexyl Urea
DEPT	Distortionless Enhancement by Polarization Transfer
DMAP	*N,N*-dimethylaminopyridine
EDC	1-(3-Dimethylaminopropyl)-3-ethylcarbodiimide hydrochloride
HETCOR	Heteronuclear Chemical Shift Correlation
HMBC	Heteronuclear Multiple Bond Correlation
HMQC	Heteronuclear Multiple-Quantum Coherence
INADEQUATE	Incredible Natural Abundance Double Quantum Transfer Experiment
NOE	Nuclear Overhauser Effect
NOESY	Nuclear Overhauser Effect Spectroscopy
TBDMS	Tetrabutyldimethylsilyl
TMS	Trimethylsilyl
TMSCl	Trimethylsilyl Chloride
TrCl	Tritylchloride

1. Introduction

Recent advances in the fermentation of glucose and improvements in synthesis and processing have positioned polylactide as a "green" alternative to petroleum-based plastics. In addition to having good mechanical properties and the processability needed for applications such as fibers and packaging materials, polylactides offer two important advantages over materials derived from petroleum. The monomer is derived from the fermentation of starch, a renewable material, and the polymer degrades to lactic acid, an environmentally benign product. Cost is the main constraint for widespread use of biodegradable materials in packaging. Petroleum-based polymers, such as polyethylene, cost about \$0.16/pound,[1] whereas polylactide is projected to be priced between \$0.50 and \$0.75/pound.

Historically, polylactide was produced for use in medical applications to take advantage of its biocompatibility. Polylactide is non-toxic and degrades *in vivo* to benign products. Polylactide and other biodegradable polymers have been used since the 1960s as resorbable synthetic sutures because they can be processed to give strong filaments that degrade rapidly. Degradable polymers also have important time-release applications in medicine as well as in the veterinary and agrochemical fields. Active ingredients ranging from pesticides to contraceptives can be delivered by sustained release from polylactide followed by the ultimate biodegradation of the carrier medium.

Lactic acid has one chiral center, and thus there are three different cyclic dimers of lactic acid. Termed lactides, L-lactide and D-lactide are enantiomers

and contain lactic acid residues with *S,S* and *R,R* stereochemistry respectively, while D,L-lactide, often termed *meso*-lactide, has *R,S* stereochemistry (Scheme 1.1). A 1:1 mixture of L-and D-lactide is termed racemic or *rac*-lactide.

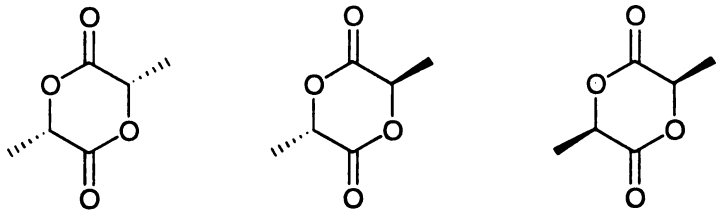

L-Lactide *meso*-Lactide D-Lactide

Scheme 1.1. Lactides

In polymers, the stereochemical configuration refers to the relative handedness of successive monomer units. Taticity in polymers refers only to the *relative* configurations of the stereocenters (e.g. R or S) along the polymer chain and are not related to the physical (up or down) orientations of the groups with respect to the polymer chain (Figure 1.1). Atactic polymers have a completely random sequence of stereocenters, syndiotactic polymers have perfectly alternating stereocenters, and isotactic polymers have identical stereocenters. A configurational sequence of two chiral centers is termed a diad, three chiral centers a triad, four centers a tetrad, and so on.

The regularity of the arrangement of the stereocenters in the polylactide chain strongly influences the properties of polymers. A random arrangement of stereocenters results in amorphous polylactide with a T_g near 60 °C, while crystalline polylactides are obtained when the stereocenters are arranged in a regular pattern, as is found in chains where the stereocenters are identical (isotactic), or alternate (syndiotatic). Stereoregular polylactide has a T_m near 180

°C, but incorporation of *rac*-lactide in crystalline polylactide inhibits crystallization and leads to a rapid decrease in tensile strength and degradation rate.[2] Therefore, full characterization of a polymer requires an analytical method for determining its microstructure.

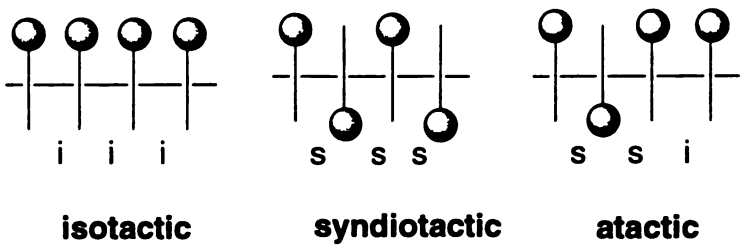

Figure 1.1. Stereochemical configuration of polymers.

1.1 Propagation Mechanisms and Models

The microstructure of polymer chains depends on the mechanism that governs the growth of the polymer. If the propagation mechanism is known, then a partial assignment of the resonances may be obtained by comparing the observed NMR intensities with those calculated from propagation models. Conversely, the propagation mechanism can be extracted by assigning the resonances and comparing the peak intensities with those predicted by propagation models.

There are several simple models for the propagation of polymer chains,[3] with each differing in how the existing microstructure of a growing chain influences the addition of the next monomer unit to the chain. The Bernoulli, or zero-order Markov model, assumes that each monomer addition is a random occurrence, and is insensitive to previous monomer addition reactions (Figure 1.2).

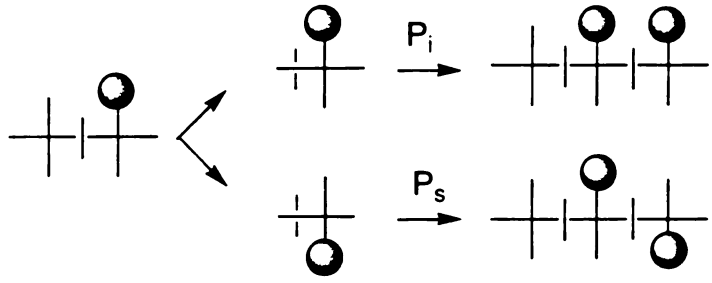

Figure 1.2. Bernoullian addition.

For a stereosequence of length *n*, Bernoullian addition leads to $2^{(n-1)}$ possible combinations of pairwise relationships that can be observed in NMR spectra. For example there are 2^2=4 possible combinations for triads, 2^3=8 possible combinations for tetrads and so on. Stereosensitivity to triads, tetrads, and pentads should give rise to 4, 8, and 16 components in the NMR spectra, respectively, for the case of Bernoullian addition of monomers to a growing chain end. In polylactide, where each monomer contains two stereocenters, Bernoullian pair-wise addition leads to patterns with 3, 5, and 7 lines, respectively.

Higher order Markov models assume that the end of a growing chain influences the addition of the monomer unit. In the first order Markov model, only the last monomer added influences addition of the next monomer unit, while the second-order Markov model considers the relative configuration of the last three psuedoasymmetric centers of the growing polymer chain (Figure 1.3).[3]

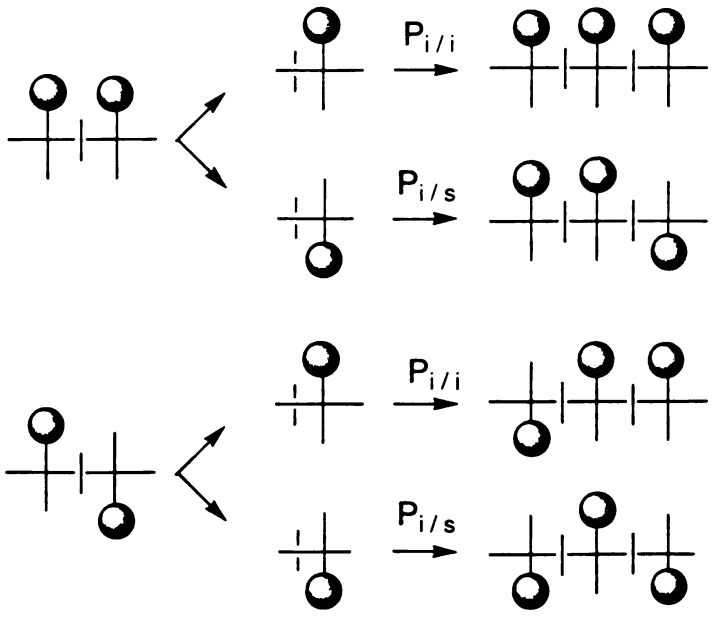

Figure 1.3. First order Markov addition.

Experimentally, it has been found that most propagating species that deviate from Bernoullian statistics have a "block-like" configuration to varying degrees. This behavior is especially common in ionic polymerizations. Coleman and Fox proposed that "block" configurations are generated in ionic polymerizations because the propagating chain end may exist in two (or possibly more) states, corresponding to chelation by the counter ion and interruption of this chelation by solvation. The Coleman-Fox model disregards any influence of the chain-end stereochemistry on the mode of addition of the next monomer unit.[3]

A polymer can be shown to be consistent or inconsistent with a given model at a given level of sequence discrimination.[3] From dyad information alone, any mechanism can be fitted but none can be tested. Using triad information, a Bernoulli model can be tested and Markov models of any order can be fitted. First-order Markov models can be tested using tetrad information, and higher

orders fitted. These statements can be extended to longer sequences. There are some limitations to the testing process. Various propagation models often predict approximately equal amounts of two or more stereosequences and often the models cannot be distinguished on the basis of intensity alone. In addition, the intensities of some of the peaks can be very small and difficult to observe in spectra. Therefore, a complete and unambiguous assignment of resonances cannot be done by this method alone.

1.2 Microstructure of Polymers

The microstructure of a polymer refers to those features of polymer chains which are fixed by their covalent structure, and is generally understood to include regioisomerism, stereochemical configuration, geometrical isomerism, branching and cross-linking.[3] In the NMR spectra of polymers, peaks that correspond to the different microstructures can be resolved, providing a detailed and quantitative characterization of chain microstructure. Polymers such as polypropylene or poly(propylene oxide) (Scheme 1.2) exhibit NMR resonances

Polypropylene Poly(propylene oxide)

Scheme 1.2. Polypropylene and poly(propylene oxide)

due to regioisomerism, as well as stereochemical configuration. In these polymers, the incoming monomer unit can add to the growing polymer chain in a head-to-tail, head-to-head, or tail-to-tail orientation as shown in Figure 1.4. The

additional resonances due to regioisomerism greatly complicate the ^{1}H NMR spectrum. ^{13}C NMR generally offers the potential for greater spectroscopic resolution and is better suited for the analysis of polymer microstructure.

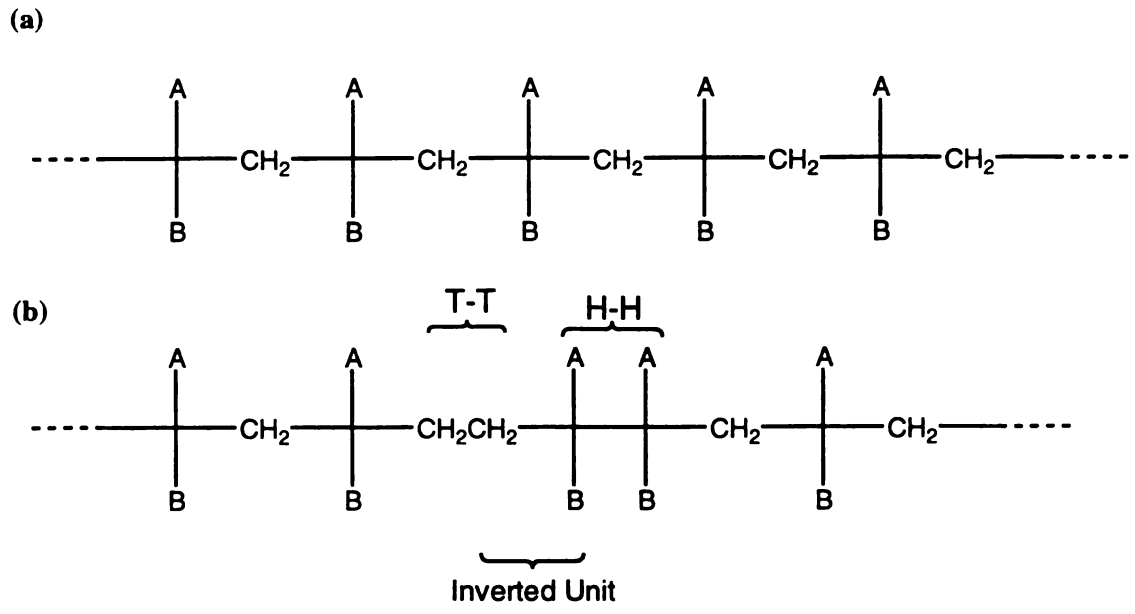

Figure 1.4. An illustration of (a) head to tail junctions and (b) tail-to-tail (T-T) and head-to-head (H-H) junctions in polypropylene.

The polymerization of diene monomers can produce structures having combinations of geometrical and stereochemical isomerism. 1,4-enchainment of polybutadiene can be either *cis* (Z) or *trans* (E) as shown in Figure 1.5. The 1,2-structures occur in isotactic or syndiotactic sequences.

Assigning the microstructures of polymers can be challenging. Comparing polymer spectra with those of model compounds or model polymers was one of the first methods used to establish NMR assignments. This approach has been very effective, but requires the precise synthesis and isolation of many compounds. Empirical chemical shift rules have been devised to identify peaks

based on the correlation between the expected chemical shift and peak intensities.

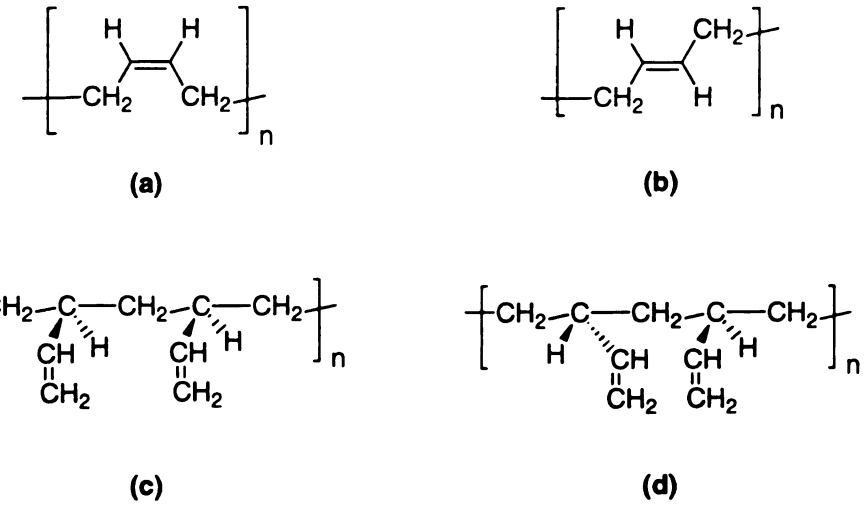

Figure 1.5. Geometrical isomerism in polybutadiene. 1,4-enchainment can be either (a) cis (Z) or (b) trans (E). 1,2-enchainment can occur in an (c) isotactic or (d) syndiotactic sequence.

1.3 Empirical Chemical Shift Rules

The chemical shifts of carbon nuclei are sensitive to their neighboring substituents. Carbon substituents α and β to an observed carbon nucleus produce comparable deshielding (~9 ppm), relative to an unsubstituted carbon.[4] The γ substituents shield the carbon nucleus with a magnitude that depends on the distance between the observed carbon and the γ substituent. Unlike the α and β effects, the γ-effect is a shielding effect and dependant on molecular conformation.[5] The determination of polymer microstructure has been facilitated by comparing the calculated chemical shifts to those of the polymer.

For those structures in which large differences in chemical shift are expected, it is possible to compare the observed chemical shifts with those

calculated on the basis of empirical rules established in small molecules. An example of such a model was developed by Breitmaier for the calculation of chemical shifts in saturated hydrocarbons.[6] The chemical shift, δ_c, is given by:

$$\delta_c = B + \Sigma A_l n_l + \Sigma S_l \qquad (1)$$

where B is the chemical shift of methane (-2.3 ppm), n_l is the number of carbons at position l away from the carbon of interest, A_l is the additive shift due to carbon l, and S_l is a term included to account for branching. The shift parameters A_l are given in Table 1.1 for the α to ε carbons. It is interesting to note that although the γ carbon is far from the carbon of interest, it still has an effect on the chemical shift. Application of this method can be illustrated by calculating the carbon chemical shift for the third carbon in 2-methyl hexane.[6]

TABLE 1.1. Parameters For Calculating the ^{13}C NMR Chemical Shifts of Alkanes Using Empirical Additivity Relationships[6]

Carbon Position	A_l ($\pm$0.10 ppm)
α	9.1
β	9.4
γ	-2.5
δ	0.3
ε	0.1

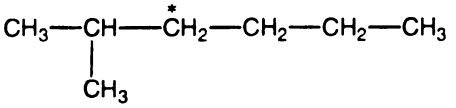

2-Methylhexane

This carbon has two α, three β, and one γ neighbor, and is a 2° carbon next to a 3° carbon (which contributes a corrective factor of –2.5), so the chemical shift calculated from Table 1.1 is:

$$\delta_C = B + 2A_\alpha + 3A_\beta + A_\gamma + S[2^o(3^o)]$$

$$= -2.3 + 18.2 + 28.2 - 2.5 - 2.5$$

$$= 39.1,$$

which may be compared with the observed value of 39.45 ppm. The idea of using a mathematical model to predict chemical shifts will be very useful in predicting the chemical shifts of polylactide.

1.4 Microstructure of Polypropylene

The aforementioned methods have been used to establish the regioisomer assignments in polypropylene.[3] Since polypropylene's chemical structure is analogous to polylactide, techniques used to determine the microstructure of polypropylene can be extended to polylactide. Polypropylene is a commercially important material, and its synthesis by some synthetic routes is known to produce polymers that contain regiodefects. Since the properties of the polymer depend on the distribution and nature of the defects, it is important to know how those defects may arise. Assigning the ^{13}C NMR resonances in polypropylene is

hampered by the overlap of many signals in the methine and methylene region as well as the possibility of stereochemical isomerism and regioisomerism.

A simple way to assign the resonances in the NMR of atactic polypropylene is to compare the NMR spectra of regioregular polypropylene to that of regioirregular polypropylene (Figure 1.6). A sample of isotactic polypropylene has a relatively simple ^{13}C NMR, with only three resonances, one for each type of carbon. Syndiotactic polypropylene has a slightly more complicated spectrum. The spectrum of atactic polypropylene can be compared to those from the isotactic and syndiotactic samples, and resonances in the atactic sample can be assigned accordingly. However, this method is limited because only a small number of resonances can be assigned. Several other methods were used to assign the remaining resonances.

In an early example, Zambelli *et al.* used heptamethyl heptadecane model compounds labeled at the 9 position to assign the resonances in the polypropylene spectrum.[7] Based on empirical observations, a mathematical model like the one developed by Breitmaier was devised to assign the resonances in polypropylene. This model incorporated calculations for a variety of microstructures. Figure 1.7 shows the complete assignment of the resonances in the 100 MHz ^{13}C spectrum.[8]

Because of the complexity of the one-dimensional spectrum, two-dimensional NMR has been used to further identify the resonances of polypropylene. Several two-dimensional experiments are particularly useful for defining polymer structure. A COSY spectrum (a two dimensional spectrum that

correlates hydrogens on adjacently bonded carbons) proved insufficient for making a complete assignment of the polypropylene spectrum because the resonances were too close together to provide meaningful data. However, the ^{13}C NMR spectrum was less complicated.

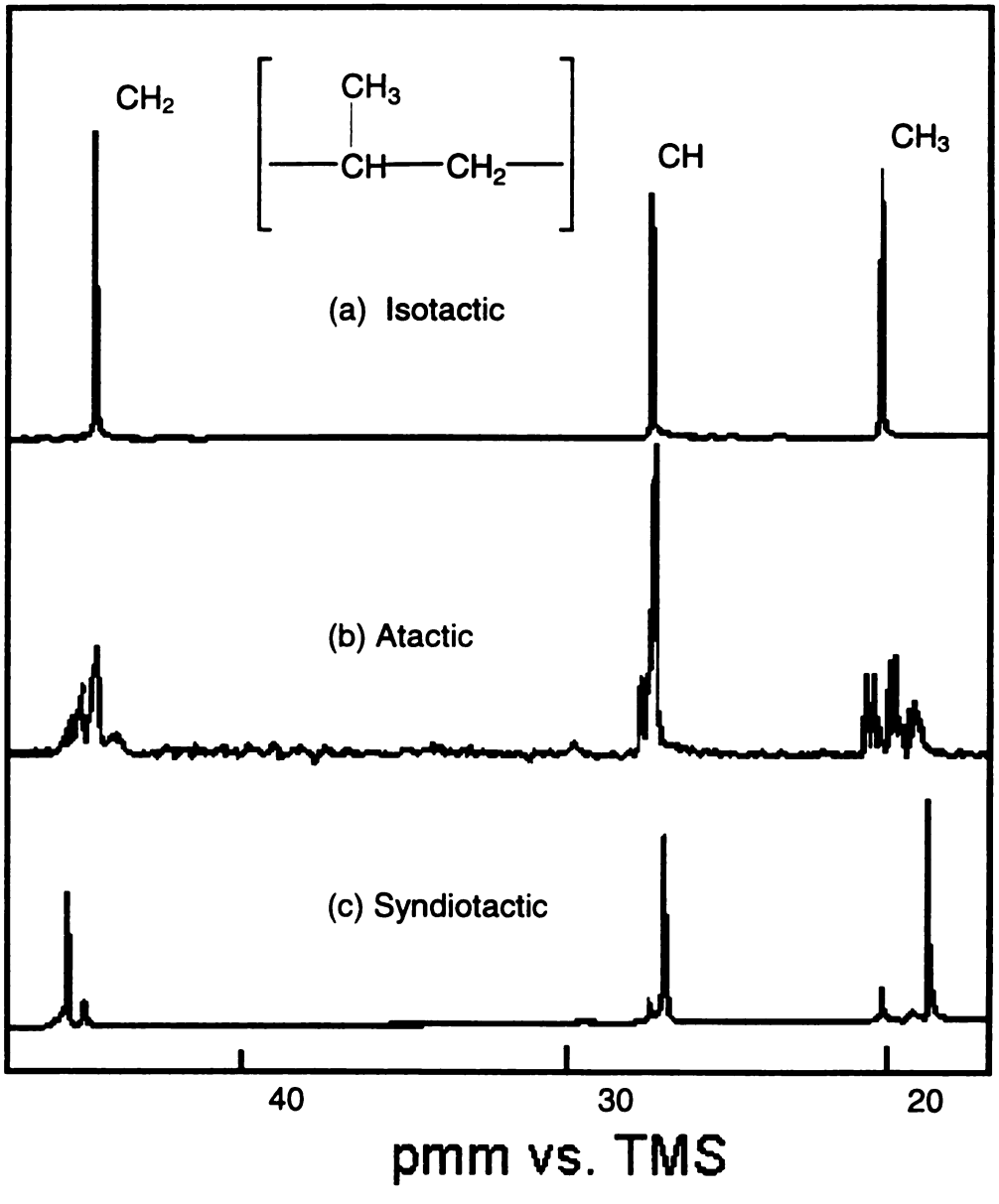

Figure 1.6. Comparison of the 25-MHz ^{13}C NMR of (a) isotactic; (b) atactic; (c) syndiotactic polypropylene. Reprinted with permission. [9]

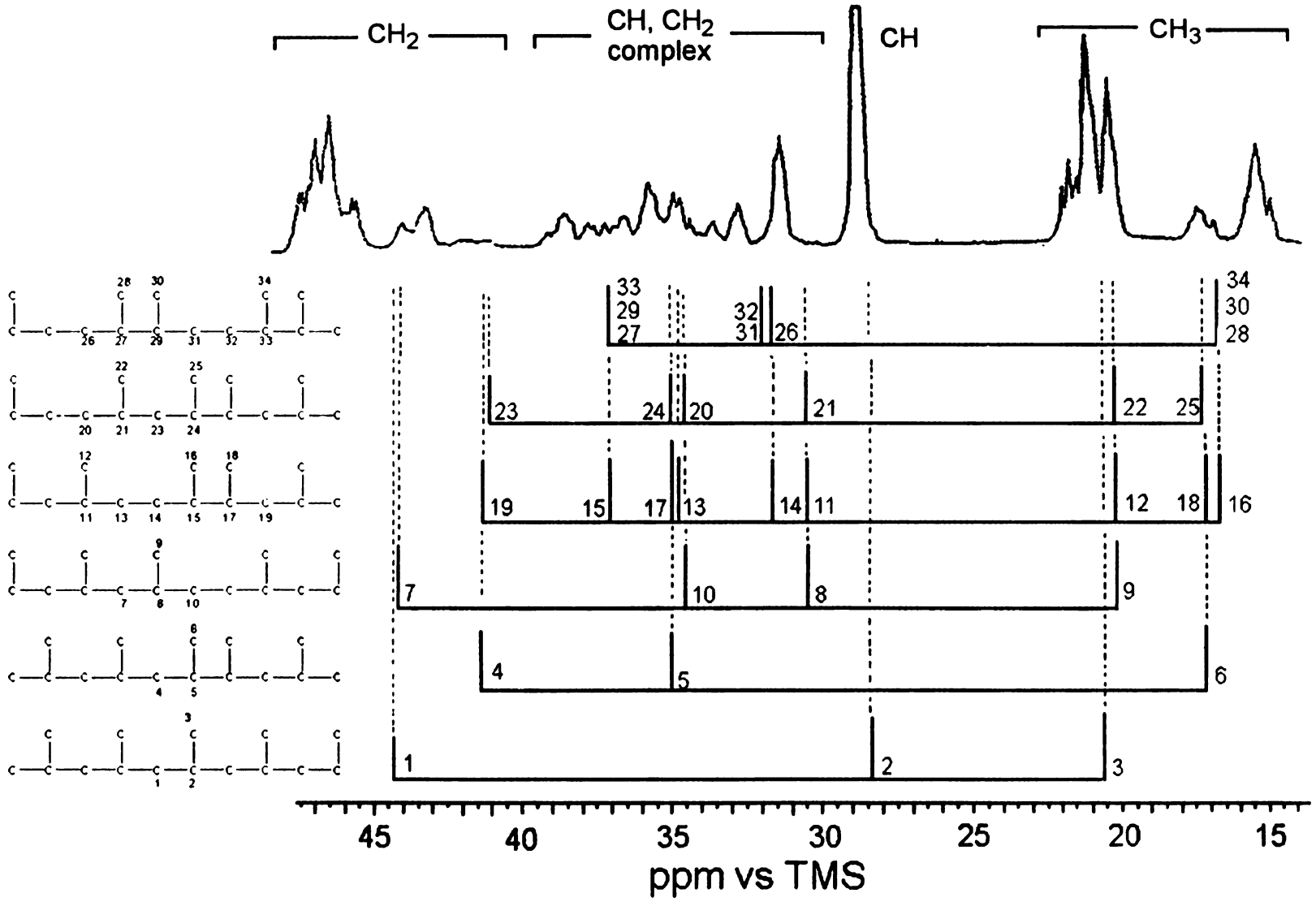

Figure 1.7. Comparison of the 100 MHz carbon spectrum of regioirregular polypropylene with the chemical shifts calculated for a variety of microstructures. Reprinted with permission.[8]

A two-dimensional INADEQUATE experiment (correlates directly bonded carbon atoms) was used to make the final assignments. The sensitivity of the INADEQUATE spectrum is greatly reduced because the odds of having two ^{13}C atoms adjacent to each other is about 10,000 times less than for protons. In spite of these difficulties, it was possible to trace the chain connectivities and assign the resonances in polypropylene.

1.5 Microstructure of Poly(propylene oxide)

Poly(propylene oxide) is another polymer that has been extensively analyzed by ^{13}C NMR, in terms of both its stereochemistry[9] and its regioisomerism.[10] Poly(propylene oxide) is a better analog to polylactide than polypropylene since poly(propylene oxide) has an oxygen in the main chain. The assignments for poly(propylene oxide) have been made primarily on the basis of chemical shift calculations and DEPT NMR spectra.[10]

1.6 Microstructure of Poly(lactide)

The microstructure of polylactide has been studied intensively in recent years. In 1975, Lillie and Schulz proposed that the ^{1}H and ^{13}C NMR spectra of polylactide were sensitive up to the triad level.[11] Various copolymers were prepared by varying the feed ratios of L- and *rac*-lactide in bulk polymerizations catalyzed by zinc dust. Lillie and Schulz observed that the relative intensities of NMR resonances decreased or increased depending on the feed ratio of L- and

rac-lactide (Figures 1.8 and 1.9). Due to significant overlap of the peaks, they were unable to conclusively assign the resonances.

Following Lillie and Schultz's report, Schindler and Harper[12] concluded that the ^{1}H NMR spectra of polymers obtained from *rac*-lactide and tin initiators such as $SnCl_4$, $SnCl_2$, stannous octoate, or tetraphenyl tin could be interpreted by applying Bernoullian polymerization statistics, and did not reflect the feed ratio of L-lactide to *rac*-lactide. They further proposed that frequency of transesterification reactions during polymerization was too low for NMR to detect the additional stereosequences that would be produced by transesterification. In contrast, Chabot and co-workers reported that transesterification was significant when they used zinc dust to polymerize various mixtures of L- and *rac*-lactide in bulk.[13] They found that the best fit of the experimental and calculated intensities of the carbonyl peaks in the ^{13}C NMR was obtained by assuming pentad sensitivity instead of triad sensitivity as proposed by Lillie and Schultz. The polymerization of *rac*-lactide should result in only seven unique pentads, and thus the carbonyl region of the ^{13}C NMR could show up to seven resonances. Through the use of resonance enhancement techniques, they observed more than seven lines in the carbonyl region, consistent with significant transesterification. Chabot and co-workers were unable to confirm the mechanism of the transesterification events, but proposed that the attack at the ester bonds in the polymer chain by active chain ends might contribute to the configurational rearrangements.

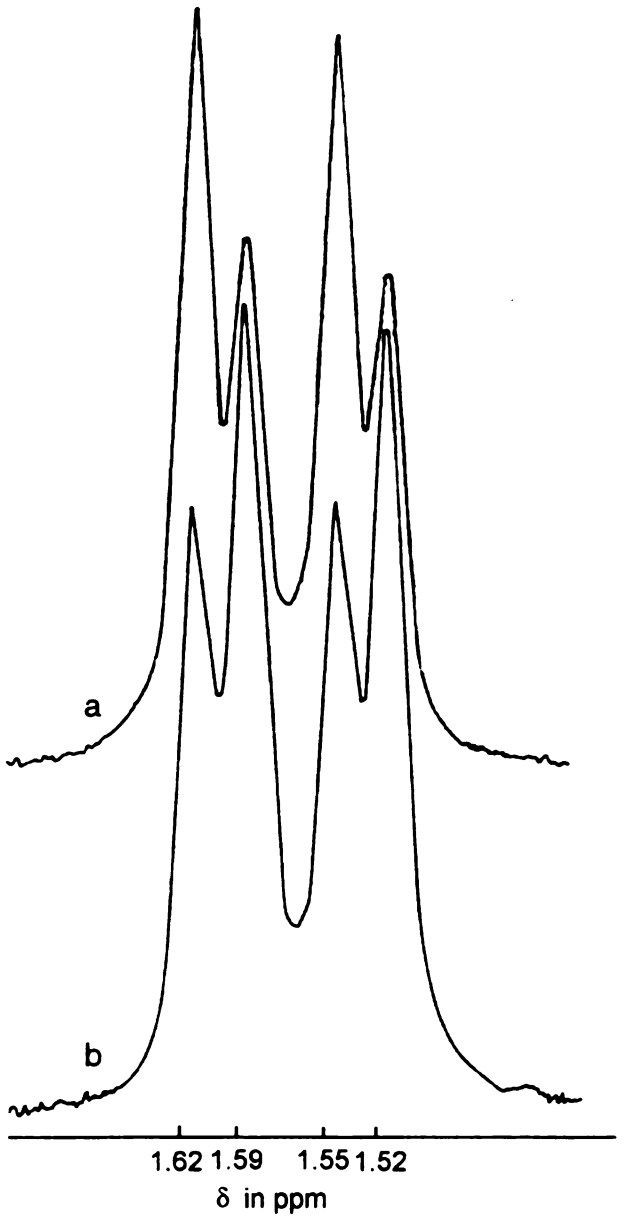

Figure 1.8. Methyl resonances from the 100 MHz ^{1}H NMR spectra of (a) polymer from 60% L-lactide with 40% *rac*-lactide; (b) polymer from 28% L-lactide with 72% *rac*-lactide. Reprinted with permission.[11]

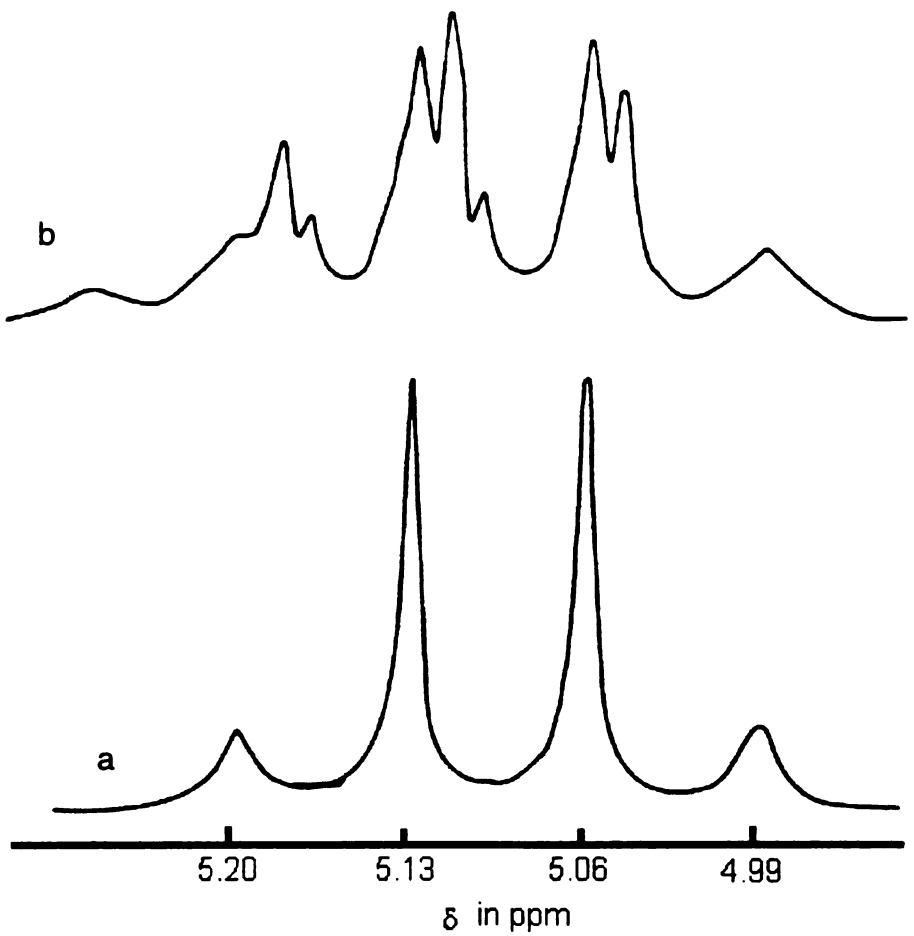

Figure 1.9. Methine resonances from the 100 MHz ^{1}H-NMR spectra of (a) poly(L-lactide); (b) polymer from 28% L-lactide and 72% *rac*-lactide. Reprinted with permission[12].

In a systematic study, Kricheldorf and co-workers improved upon the previous sequence assignments by comparing polymers obtained from the polymerization of *rac*- and *meso*-lactide with two tin initiators under identical reaction conditions.[14] Tributyltin methoxide (Bu_3SnOMe) was known to catalyze transesterification during the polymerization of L-lactide and various lactones at moderate temperatures.[14] However, Sn(II) octoate gave high molecular weight polylactides without racemization. They also evaluated the influence of the reaction time and temperature on the stereochemical course of the polymerizations.

Kricheldorf and co-workers considered more information when proposing their assignments of the NMR spectra.[14] They compared poly(D,L-lactide)s prepared from *rac*- and *meso*-lactide in the absence of transesterification and racemization of monomers or monomeric units. Polymerization at high temperatures (e.g. 180 °C) provided perfectly random stereosequences due to rapid transesterification. Copolylactides prepared by copolymerization of L-lactide with *rac*-lactide also were studied. They found that both the ^1H and ^{13}C NMR methine signals of various mixtures of poly(D,L-lactides) displayed five peaks, indicating at least tetrad level sensitivity for both signals (Figures 1.10 and 1.11).[14] Bernoullian statistics were used to assign the possible stereosequences, disregarding transesterification.

The assignments made by Kricheldorf were accepted as the correct assignments until Thakur and co-workers disclosed[15] that the ^{13}C and ^1H NMR spectra of polylactide were sensitive to the hexad level. Assignments at the

hexad level were made using homonuculear decoupling and high resolution NMR spectroscopy techniques[15] (Figures 1.12 and 1.13), in conjunction with the trends seen in the spectra with changes in the feed composition.

A debate concerning the NMR assignments arose when Chisholm and co-workers[16] contradicted the assignments proposed by Kricheldorf. Chisholm and co-workers used HETCOR to correlate the homodecoupled methine protons with the methine carbons of homodecoupled poly(*rac*-lactide) and poly(*meso*-lactide). Their HETCOR spectrum (Figure 1.14) of poly(*meso*-lactide) showed that a resonance previously assigned to the *isi* tetrad in either the ^{1}H- or ^{13}C-NMR spectrum clearly correlates with *two* resonances in the spectrum of the other nucleus. They proposed an alternative assignment of the ^{13}C and ^{1}H NMR spectra (Figure 1.15) even though their new assignments did not conform to Bernoullian statistics.

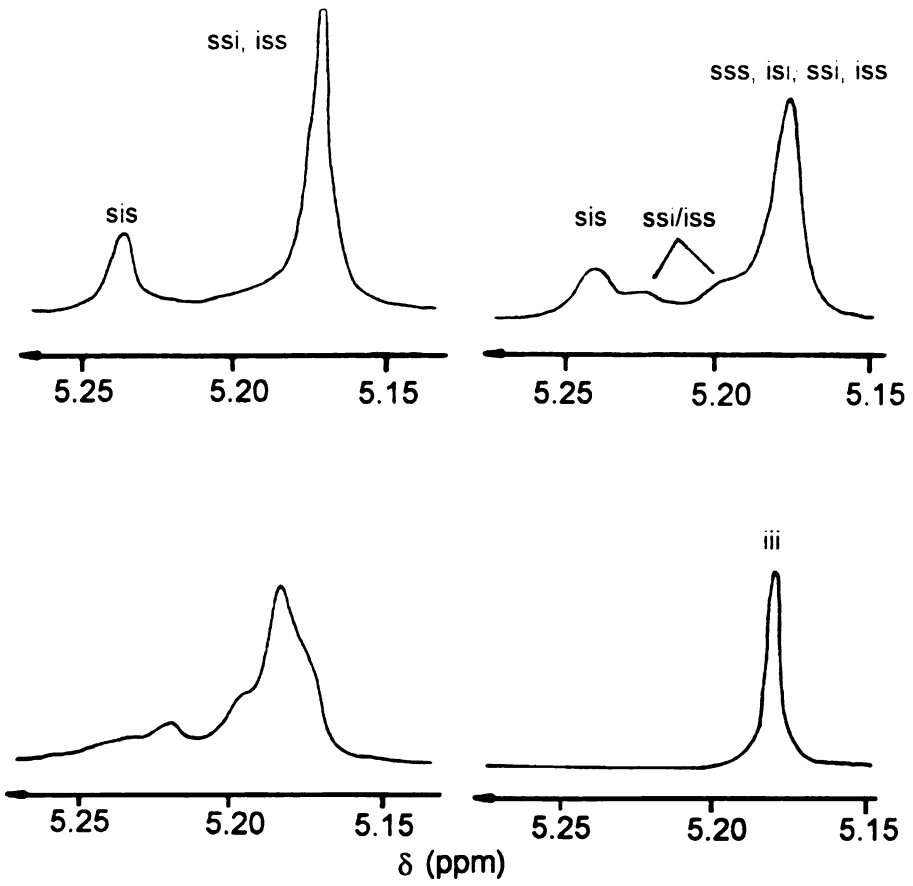

Figure 1.10. ^{1}H NMR (homodecoupled C-H signal) of *co*-poly-(D,L-lactide)s prepared from *meso* D,L-lactide and L-lactide with Sn(II) octoate: (a) poly(D_{50}, L_{50}); (b) poly(D_{40},L_{60}); (c) poly(D_{20},L_{80}); (d) poly(L-lactide). Reprinted with permission.[14]

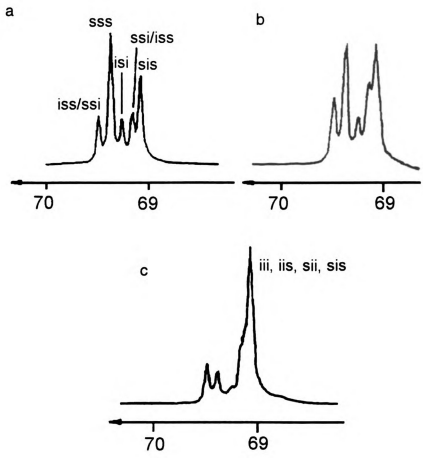

Figure 1.11. ^{13}C NMR (CH group) of *co*-poly(D,L-Lactide)s prepared from *rac*-lactide with Sn(II) octoate (a) poly(D_{50}, L_{50}); (b) poly(D_{40}, L_{60}); (c) poly(D_{20}, L_{80}). Reprinted with permission.[15]

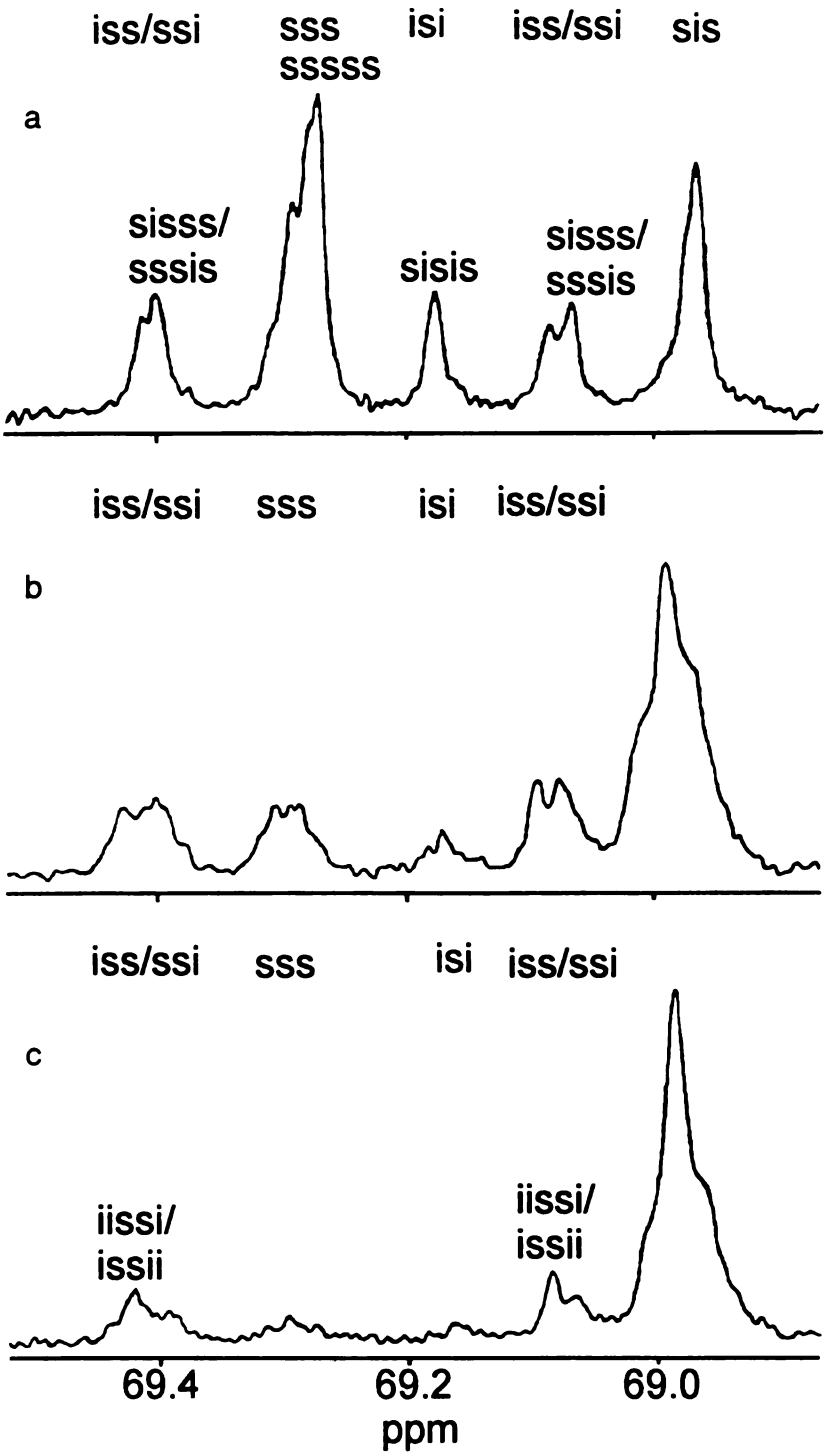

Figure 1.12. Methine resonances in the ^{13}C NMR spectra of poly(lactide) samples (a) poly(lactide) from 3% L-lactide, 3% D-lactide, 94% *meso*-lactide;(b) poly(lactide) from 51.5% L-lactide, 1.5% D-lactide, 47% *meso*-lactide; (c) poly(lactide) from 70.9% L-lactide, 0.99% D-lactide, 47% *meso*-lactide. Reprinted with permission.[15]

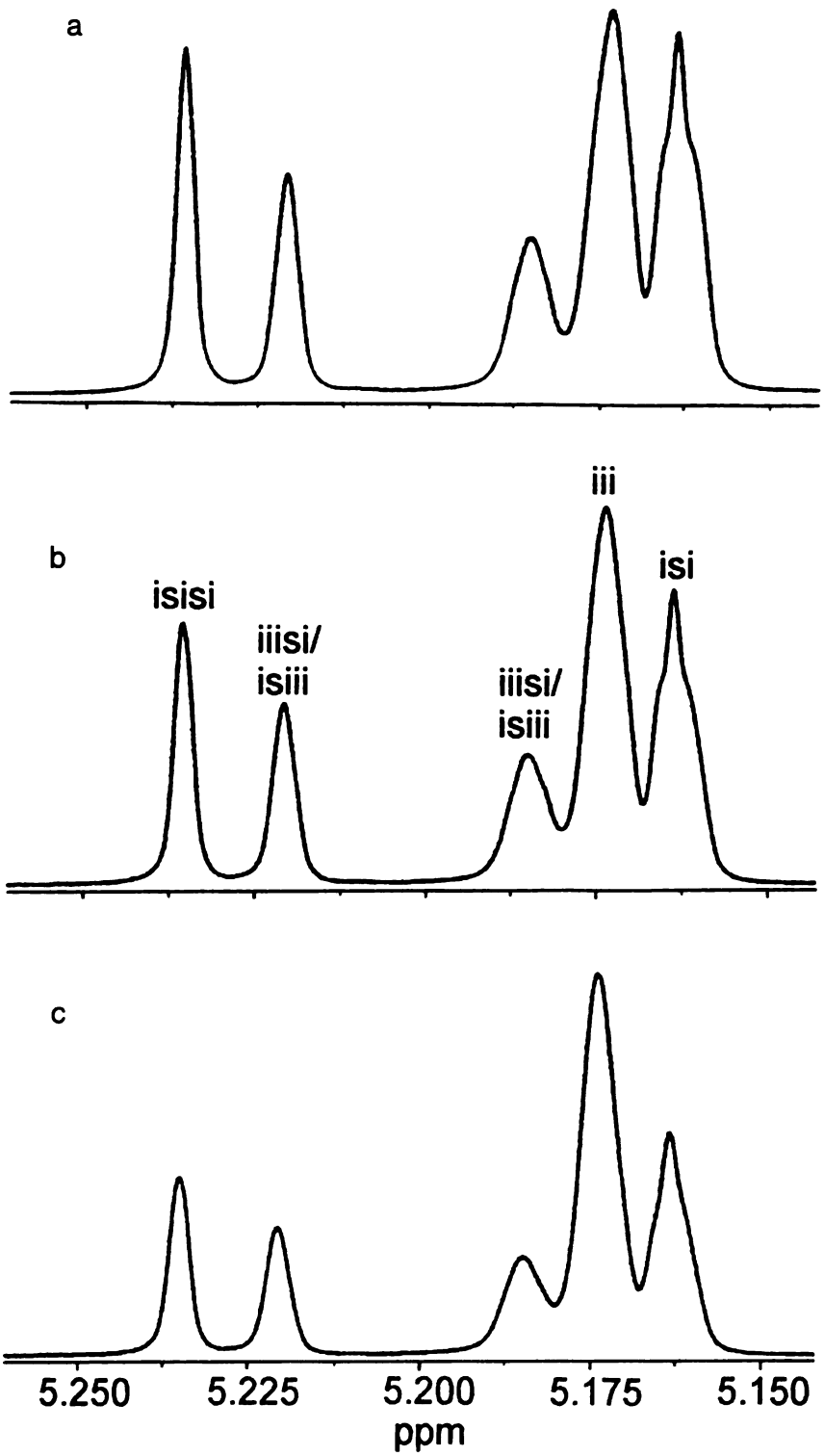

Figure 1.13. Methine resonances in the homonuclear decoupled ^1H NMR spectra of poly(lactide) samples (a) poly(D_{50}, L_{50}-lactide); (b) poly(D_{60}, L_{40}-lactide); (c) poly(D_{70}, L_{30}-lactide). Reprinted with permission.[16]

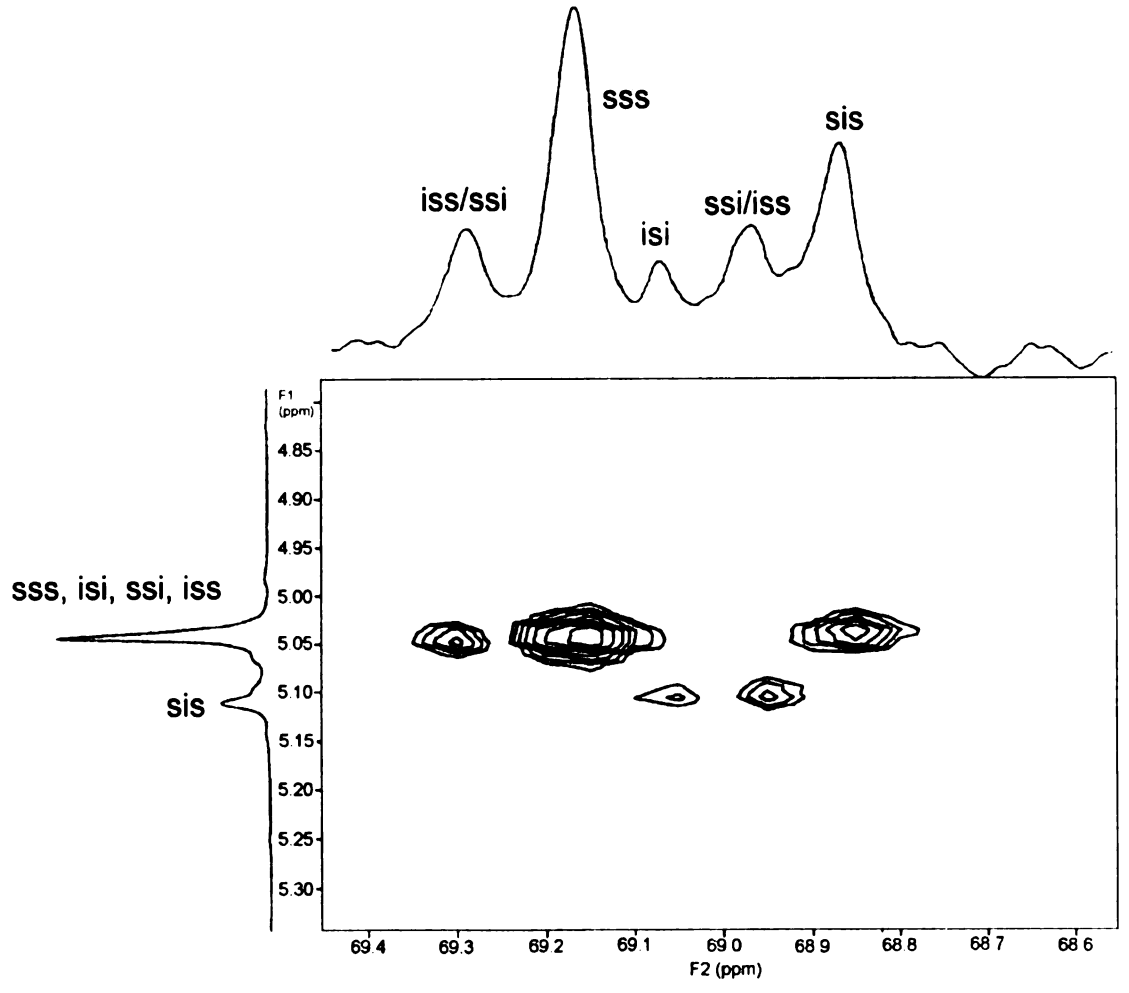

Figure 1.14. HETCOR spectrum of poly(*meso*-lactide). Reprinted with permission.[18]

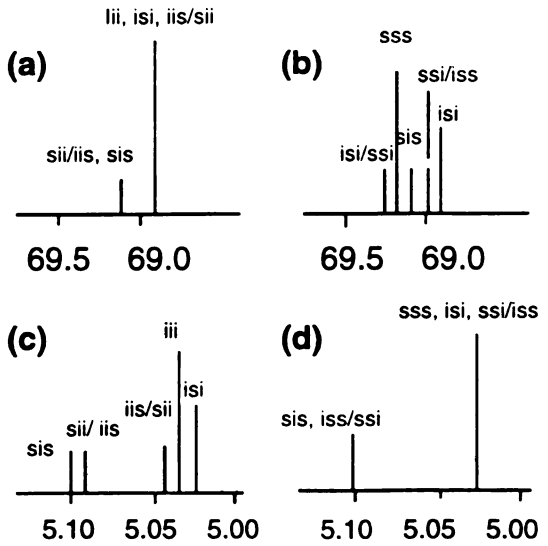

Figure 1.15. Tetrad assignments for poly(*rac*-lactide) and poly(*meso*-lactide) based on the HETCOR spectra as proposed by Chisholm. Reprinted with permission.[16]

Thakur and co-workers[17] suggested that the influence of the chiral centers adjoining the center unit of the pentad were different for ^{1}H NMR and ^{13}C NMR, thus causing the discrepancy found in HETCOR as described by Chisholm. Thakur proposed that the polylactide microstructure influences the ^{1}H NMR and ^{13}C NMR chemical shift tensors differently (Table 1.2). For example, in the stereosequence *–RRSSS-* (Figure 1.16), represented by *isii*, the chirality of the center unit is *S*. In ^{13}C NMR the chemical shift tensor of this stereocenter would be affected by the two chiral centers to the left and one stereocenter to the right, which leads to tetrad *sii*. However, in the ^{1}H NMR, the same stereocenter would be affected by one chiral center to the left and two chiral centers to the right which leads to tetrad *sis*. Therefore, the *sii* resonance in the ^{13}C NMR spectrum should have a cross-peak with the *sis* resonance in the ^{1}H NMR spectrum. The *isi* tetrad is also found in the pentad *isis* (Figure 1.16). If the chemical shift

tensors for the central chiral center are rationalized as described above, there will be a cross-peak between the *sis* tetrad and the *isi* tetrad. Therefore in the HETCOR spectrum of poly(*meso*-lactide), the *isi* tetrad in the ^{1}H NMR will have a cross peak in the ^{13}C NMR with both the *sis* and *sii* tetrads (Figure 1.14).

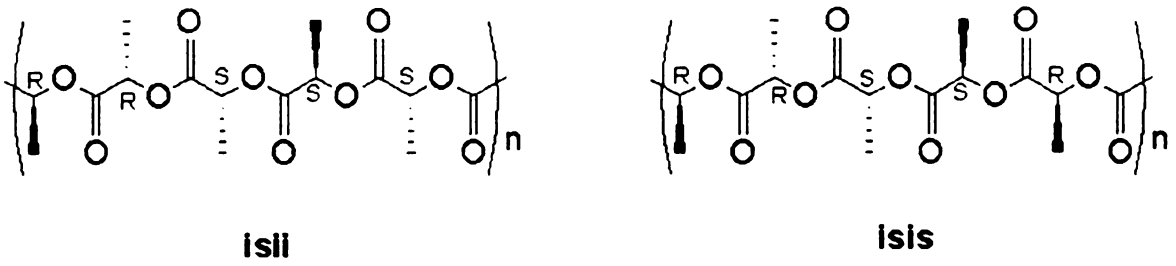

Figure 1.16. *isii* and *isis* pentads.

Table 1.2. Influence of Chiral Centers on the Chemical Shift Tensor

	Influence of Chiral Centers	Tetrad from *isii*	Tetrad from *isis*
^{13}C NMR	1 Left 2 right	*sii*	*sis*
^{1}H NMR	2 Left 1 Right	*isi*	*isi*

In questioning the validity of Thakur and co-workers assumption of chemical shift tensors propagating in opposite directions,[18] Chisholm noted that that this phenomenon is rare and only was reported by Bovey and co-workers[3] in their study of atatic poly(propylene oxide). However, the structures of poly(propylene) and poly(lactide) are indeed quite similar (Scheme 1.3), and drawing an analogy

between Bovey's findings on poly(propylene oxide) and poly(lactide) case is reasonable.

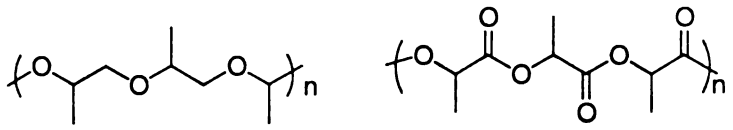

Poly(propylene oxide) Poly(lactide)

Scheme 1.3 Poly(propylene oxide) and poly(lactide)

Chisholm suggested an alternative explanation, that the observed spectral evidence can be explained in terms of next nearest neighbor effects (Table 1.3).[18] They proposed that the observed HETCOR spectra can be explained in terms of triad and pentad sensitivity and not tetrad or hexad sensitivity. They proposed that stereosequences *ii* and *ss* would show unique triad resonances, whereas heterotactic sequences *is* and *si* could be split by neighboring effects to yield resonances that correlate with pentad sensitivity. Thus the *is* triad would give rise to *iisi*, *iiss*, *siss*, and *sisi* pentads. The *iisi* and *sisi* pentads could come from poly(*rac*-lactide),while the *siss* and *sisi* pentads could arise from poly(*meso*-lactide). Pentad *iiss* can only come from atactic polylactide.

Table 1.3. Next-Nearest Neighbor Effects

Possible Triads		Pentad		Origin
ii	RRR	Not affected		*rac*-lactide
ss	RSR	Not affected		*meso*-lactide
is	RRS	*iisi*	RRRSS	*rac*-lactide
		iiss	RRRSR	atactic
		siss	RSSRS	*meso*-lactide
		sisi	RSSRR	*meso*- or *rac*-lactide
si	RSS	*ssis*	RSRRS	*meso*-lactide
		ssii	RSRRR	atactic
		isis	RRSSR	*rac*-lactide
		isii	RRSSS	*rac*-lactide

The HETCOR spectra (Fig. 1.17) of atatic poly(lactide) should show all possible pentad sequences and at least one should produce a new cross peak due to the pentads (*iiss* and *ssii*) from atactic polylactide. Chisholm and co-workers felt the appearance of a new peak in the HETCOR spectra (Figure 1.17) supported their hypothesis and discredited the hypothesis of Thakur and co-workers.

The application of the Bernoulli model to describe the propagation of the polymer chain has been questioned by Kasperczyk, Thakur and others. In his study of the lithium *tert*-butoxide initiated polymerization of *rac*-lactide, Kasperzyk noted that the NMR intensities from the syndiotactic sequences were higher than would be expected for Bernoullian addition.[19] Thakur found that when Sn(II)

octoate was used as the initiator, the stereospecificity of lactide polymerization changed over time.[20]

NMR study of polylactide model compounds may conclusively determine the chemical shifts of the different microstructure of polylactide. Due to the connectivity of lactide, the polymer cannot have regio- or geometrical isomers, and thus the NMR spectrum will only show resonances due to stereoisomers. Polylactide hexads with known stereochemistry were synthesized using an iterative procedure. Each hexad had unique ^{13}C and ^{1}H NMR spectra, that were assigned based on trends in the spectra as well as comparison to the spectra of smaller oligomers. A method similar to the empirical chemical shift relationships used to assign the chemical shifts of poly(propylene) and poly(propylene oxide), was developed from analysis of the NMR spectra of poly(lactide) hexads.

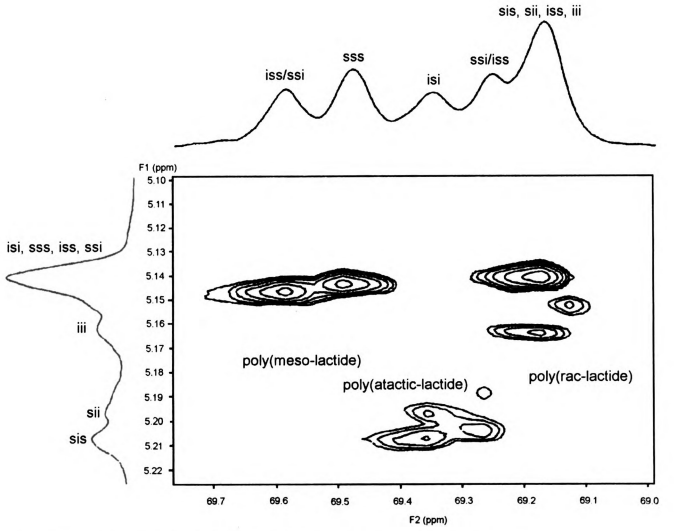

Figure 1.17. HETCOR spectrum of atactic poly(lactide). Reprinted with permission.[18]

References

1. Bozell, J. J. *Chemicals and Materials from Renewable Resources*; American Chemical Society: Washington D.C.

2. Vert, M. *Macromolecular Biomaterials*; CRC Press:, 1986.

3. Bovey, F. A.; Mirau, P. A. *NMR of Polymers*; 2 ed.; Academic Press, Inc.: San Diego, CA, 1996.

4. Stehling, F. C.; Knox, J. R. *Macromolecules* **1975**, *8*, 595-603.

5. Grant, D. M.; Cheney, B. V. *J. Am. Chem. Soc.* **1967**, *89*, 5315.

6. Breitmaier, E.; Voelter, W. *Carbon-13 NMR Spectroscopy*; 3 ed.; Weinheim:, 1987.

7. Zambelli, A.; Locatelli, P.; Bajo, G.; Bovey, F. A. *Macromolecules* **1975**, *8*, 687.

8. Asakura, T.; Nakayamma, N.; M.Demura; Asano, A. *Macromolecules* **1992**, *25*, 4876.

9. Tonelli, A.; Schilling, F. *Acc. Chem. Res.* **1981**, *14*, 233.

10. Shilling, F. C.; Tonelli, A. E. *Macromolecules* **1986**, *19*, 1337.

11. Lillie, E.; Schulz, R. C. *Die Makromlekulare Chemie* **1975**, *176*, 190-1906.

12. Schindler, A.; Harper, D. *Polymer Letters* **1976**, *14*, 729-734.

13. Chabot, F.; Vert, M.; Chapelle, S.; Granger, P. *Polymer* **1983**, *24*, 53-59.

14. Kricheldorf, H. R.; Boettcher, C.; Tonnes, K.-U. *Polymer* **1992**, *33*, 2817-2824.

15. Thakur, K. A. M.; Kean, R. T.; Hall, E. S.; Kolstad, J. J.; Lindgren, T. A. *Macromolecules* **1997**, *30*, 2422-2428.

16. Chisholm, M. H.; Iyer, S. S.; Matison, M. E.; McCollum, D. G.; Pagel, M. *Chemical Communications* **1997**, 1999-2000.

17. Thakur, K. A. M.; Kean, R. T.; Zell, M. T.; Padden, B. E.; Munson, E. J. *Chemical Communications* **1998**, 1913-1914.

18. Chisholm, M. H.; Iyer, S. S.; McCollum, D. G.; Pagel, M.; Werner-Zwanziger, U. *Macromolecules* **1999**, *32*, 963-973.

19. Bero, M.; Dobrzynski, P.; Kasperczyk, J. *Journal of Polymer Science: Part A: Polymer Chemistry* **1999**, *37*, 4308-4042.

20. Thakur, K. A. M.; Kean, R. T.; Hall, E. S.; Kolstad, J. J.; Munson, E. *Macromolecules* **1998**, *31*, 1487-1494.

2. Discussion

The notion of studying low molecular weight model compounds to better understand the properties of polymers is a well-established strategy, especially for clarifying the stereochemical relationships in polymers. Since Thakur and Kricheldorf assigned the ^{1}H and ^{13}C NMR of poly(lactide) to the hexad level (six repeating units),[1,2] compounds that contain six lactic acid residues should be good model compounds for poly(lactide). Hexads were synthesized using an iterative procedure so that the exact stereosequence of each hexad would be known. Ideally, the ^{1}H and ^{13}C NMR spectra for each hexad would be identical to the same hexad embedded in the poly(lactide) chain. However, the hexads are short linear compounds, and thus the chain ends have a large effect on the chemical shift of each carbon atom in the hexad. The magnitude of the "end effect" on the chemical shift of each lactic acid residue in the hexad can be estimated by comparing the chemical shifts of the all-isotactic hexad with the spectrum of poly(L-lactide).

There are 32 possible hexads (Table 2.1), and since the isotactic and syndiotactic relationships in polymers are based on the relative stereochemistry of the chain, only one enantiomer of each hexad must be synthesized to establish the stereochemical assignments. The synthesis of the hexads used an iterative series of esterification reactions (Scheme 2.1) to grow the hexad from an anchoring block. Initially, the commercially available and inexpensive *S*-ethyllactate was evaluated as the anchoring block for each hexad. However, the chemical shift of the methylene hydrogens of the ethyl ester group was similar to

that of the lactic acid methine proton, which could complicate the process of making NMR assignments for the hexads. Since the spectrum of the methyl ester of *S*-lactic acid shows less interference, the strategy was modified to use *S*-lactic acid methyl ester as the anchor for each hexad. S-methyl lactate was obtained in 93% yield from the HCl-catalyzed methanolysis of L-lactide (Scheme 2.2). Running the reaction in the absence of HCl gave the methyl ester of the *S,S* dimer in 96% yield, a particularly useful anchor block for the synthesis of hexads that start with an S,S sequence.

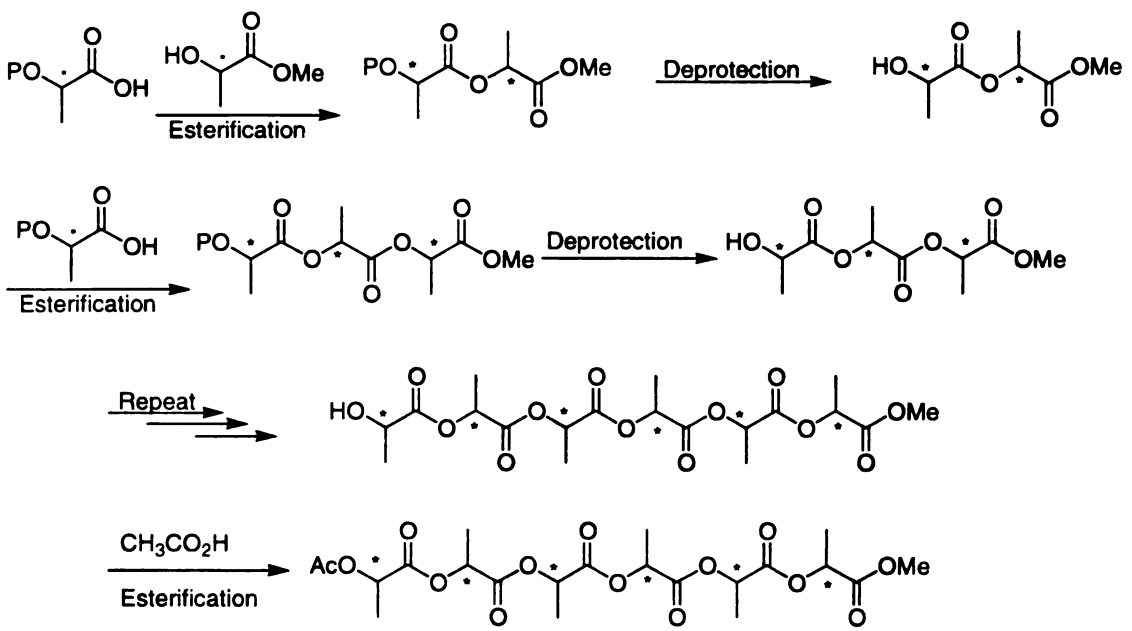

Scheme 2.1. Synthetic route to poly(lactide) hexads.

Table 2.1. The 32 possible Hexads

Tacticity	Hexad	Enantiomer	Tacticity	Hexad	Enantiomer
issss	SSRSRS	RRSRSR	*ssiii*	SRSSSS	RSRRRR
sisss	SRRSRS	RSSRSR	*iissi*	SSSRSS	RRRSRR
ssiss	SRSSRS	RSRRSR	*isiss*	RRSSRS	SSRRSR
sssis	SRSRRS	RSRSSR	*sisis*	RSSRRS	SRRSSR
ssssi	SRSRSS	RSRSRR	*ssisi*	RSRRSS	SRSSRR
siiii	RSSSSS	SRRRRR	*sisii*	SRRSS	RSSRRR
isiii	RRSSSS	SSRRRR	*isisi*	SSRRSS	RRSSRR
iisii	RRRSSS	SSSRRR	*iisis*	SSSRRS	RRRSSR
iiiis	RRRRRS	SSSSSR	*sissi*	RSSRSS	SRRSRR
sssii	RSRSSS	SRSRRR	*isssi*	RRSRSS	SSRSRR
siiss	RSSSRS	SRRRSR	*siisi*	SRRRSS	RSSSRR
iisss	RRRSRS	SSSRSR	*isiis*	SSRRRS	RRSSSR
ssiis	RSRRRS	SRSSSR	*siiis*	SRRRRS	RSSSSR
iiiss	SSSSRS	RRRRSR	*sssss*	RSRSRS	SRSRSR
issii	SSRSSS	RRSRRR	*iiiii*	SSSSSS	RRRRRR

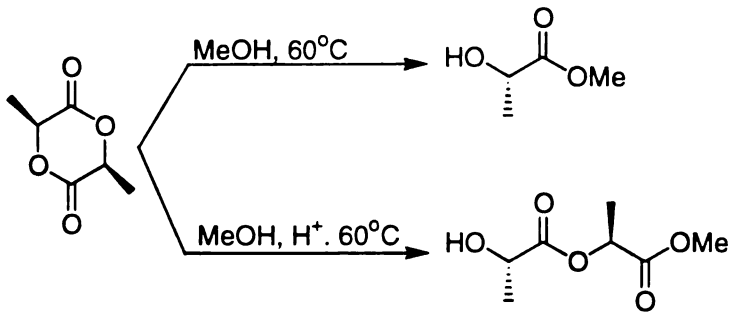

Scheme 2.2. Methanolysis of L-lactide

To ensure that esterification took place in a predictable manner, each lactic acid residue was added in the form of lactic acid with a protected hydroxyl group and a free carboxylic acid. The ideal protecting group must be robust enough to withstand the conditions of the esterification reaction, but be easily removed. An added complication is that for purification reasons, esters were used as substrates instead of acids, and the protecting group must also survive the ester hydrolysis reaction. Several silane-based protecting groups were evaluated (Scheme 2.3). Protection of the hydroxyl moiety with trimethylsilyl chloride (TMSCl) was easily achieved, does not interfere with the coupling chemistry, and is easily removed with tetrabutylammonium fluoride. However the TMS group partially hydrolyzed under the basic conditions used to hydrolyze the ethyl ester in a subsequent reaction. Similar results were obtained when the protecting group was switched to the tetrabutyldimethylsilyl (TBDMS) group.

Benzyl bromide offer two potential advantages as a protecting group. Removal of the benzyl group by hydrogenation would side-step the hydrolysis problems encountered with the silanes, and the addition of the benzyl group might induce crystallinity to the carboxylic acid and simplify purification of the

intermediates. As expected, the benzyl group was stable to hydrolysis, and both (R)- and (S)-2-benzyloxylpropanoic acid were crystalline solids. Tritylchloride (TrCl) was briefly considered, but the purification of the protected acid by vacuum distillation was not successful, and resulted in oligomerization.

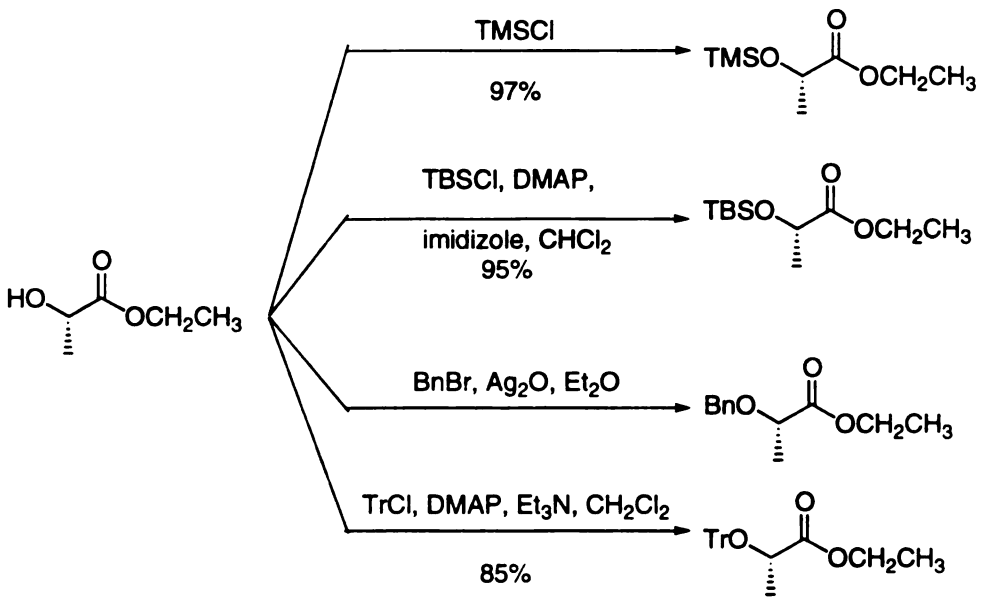

Scheme 2.3. Protecting groups tried

Ether, THF, and CH_2Cl_2 were considered as potential solvents for the protection reaction. Running the reaction in dry CH_2Cl_2 at reflux allowed smooth conversion to the benzyl ether, while using dry THF as the solvent led to an inseparable mixture. Purification of ethyl (S)-2-benzyloxypropanoate and methyl (R)-2-benzyloxypropanoate proved difficult. Vacuum distillation resulted in oligomerization, while column chromatography using silica gel as the stationary phase resulted in hydrolysis of the ester. Therefore the crude benzyl-protected ester was hydrolyzed in a 1:1 mixture of 0.2M LiOH and THF to give after work

up, ~ 60% yield of (S)-2-benzyloxypropanoic acid and (R)-2-benzyloxypropanoic acid as crystalline compounds with clean ^{1}H NMR spectra.

Carbodiimides were used to couple the benzyl-protected acids to the anchor block. Dicyclohexylcarbodiimide (DCC) gave the coupled product in high yield, but ^{1}H NMR showed that the dicyclohexyl urea (DCU) byproduct, which is sparingly soluble in CH_2Cl_2 , diethyl ether, and water could not be successfully removed from the product. The urea byproduct of 1-(3-dimethylaminopropyl)-3-ethylcarbodiimide hydrochloride (EDC), a water soluble analogue of DCC, is water soluble and was removed completely with an aqueous workup. However, the relatively low yield (~60%) of the reaction was a major drawback to using EDC.

The use of a catalytic amount of *N,N*-dimethylaminopyridine (DMAP) was necessary for the coupling reaction. When run for > 1 hour, ^{13}C NMR spectra of the coupled products showed signs of epimerization. The carboxylic acid acts as an electron withdrawing group, and due to the relatively low pK_a of the methine proton in the protected hydroxy acids, DMAP was able to abstract the methine proton from the protected acid. When run in the minimum amount of dry CH_2Cl_2 needed to dissolve EDC, no epimerization was observed for reaction times less than a half hour. It was imperative for the reaction to be run in dry CH_2Cl_2. In wet solvent, the coupling reaction was too slow to compete with the reaction of residual water with EDC. Thus, CH_2Cl_2 was dried over CaH_2 prior to use.

After coupling the benzyl-protected α-hydroxy acid to the anchor, the benzyl group was removed by hydrogenolysis. Typical conditions for such

reactions are 50 psi of H_2 in the presence of a catalytic amount of 5% or 10% palladium on carbon, often using a methanol/acetic acid solution as the solvent. It is thought that the hydrogenation mechanism involves the abstraction of a proton from the solvent, so a slightly protic solvent is needed. Under these conditions, the benzyl group was removed but the ester linkages were also hydrolyzed. Switching to CH_2Cl_2 as the solvent gave no hydrogenolysis of the benzyl ether even at 500 psi. The reaction proceeded slowly in diethyl ether at 55 psi H_2, but was much faster at 500-600 psi. The time to completion of the deprotection reaction varied widely, from as little as four hours to as much as one week. This variability is likely due to poisoning of the catalyst, since reactions run with Pd/C that had been stored on the bench top were slower than those that used Pd/C that had been stored in the dry box. Batch to batch variation also was observed for the Pd/C catalyst.

When the synthesis of the desired *n*-ad was completed, the benzylated *n*-ad was deprotected and acetylated with acetic acid. The esterification was run as before, except that acetic acid was used as the carboxylic acid. Careful attention was needed, since the coupling reaction did not proceed in an excess of acetic acid. The acetylation also required an additional equivalent of EDC, presumably due to residual water in the acetic acid. The acetylation reaction was complete in less than a half hour and gave a 60% yield of the product.

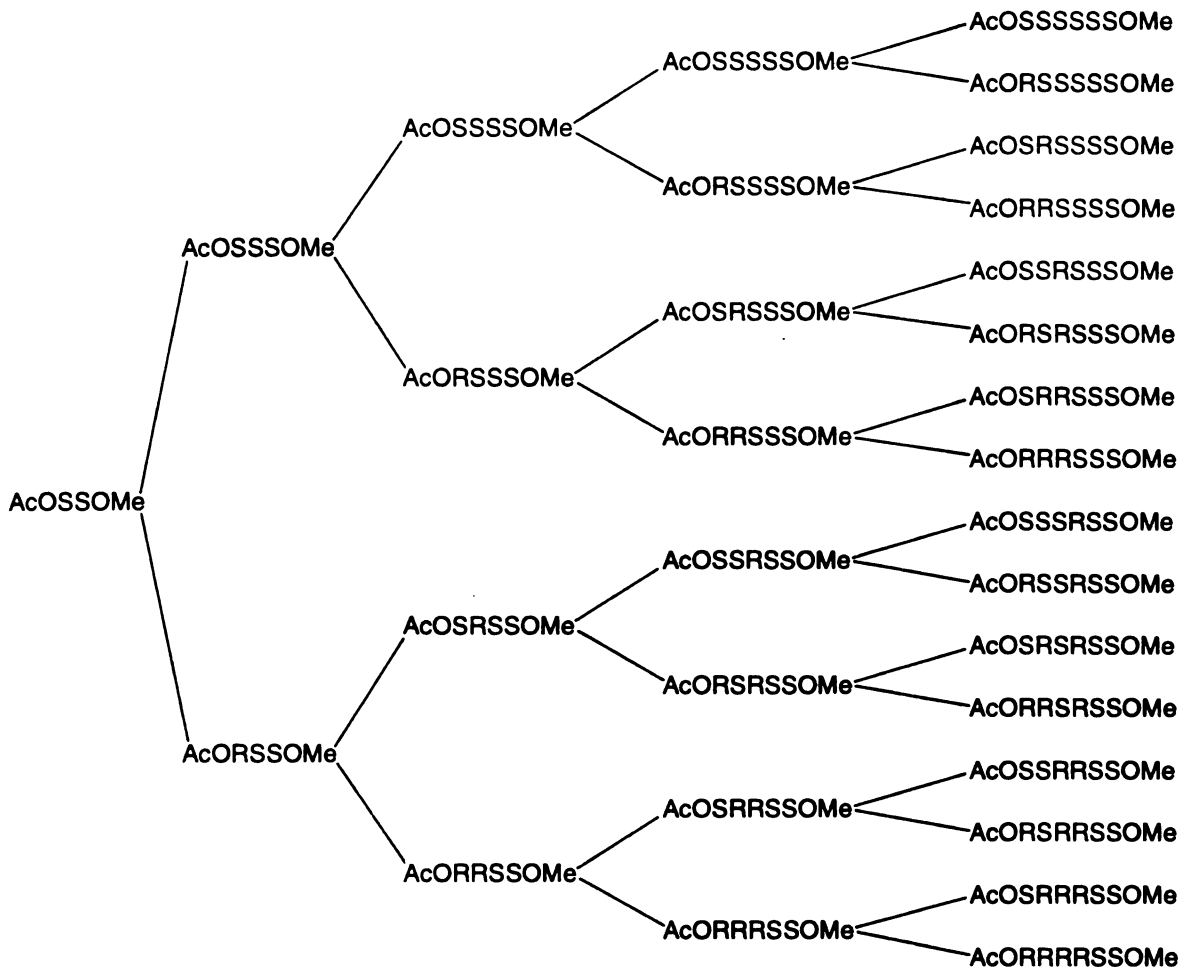

Figure 2.1. An example of synthetic methodology used to synthesize hexads.

The path to each hexad is shown in Figure 2.1. Seventeen of the 32 possible hexads were synthesized (Table 2.2), as well as smaller oligomers that were acetylated and used to help make assignments of the ^{13}C resonances. Each hexad was a clear, colorless, viscous oil. For convenience, each hexad is symbolically represented to reflect the stereochemistry of each lactic acid residue with the end groups denoted by standard abbreviations. Thus, (2R)-2-{{(2'S)-2'-{{(2"R)-2"-{{(2"'S)-2"'-{{(2""S)-2""{{(2"""S)-2"""-benzyloxypropanoyl}oxy} propanoyl}oxy}propanoyl}oxy}propanoyl}oxy}propanoyl}oxy}propanoic acid methyl ester is represented as BnORSRSSSOMe. Similarly, its acetylated

derivative is abbreviated as AcORSRSSSOMe. Each compound can also be classified according to their stereochemical relationships. Recall that "*s*" refers to a syndiotactic relationship (opposite configurations) between two adjoining stereocenters and that "*i*" refers to an isotactic relationship (same configuration) between the two adjoining stereocenters. Thus, AcORSRSSSOMe can also be represented as *sssii*, with the understanding that the hexad is always oriented with the methyl ester to the right and the acetate to the left. Using this scheme, there are two possible hexads for each sequence. For example, *sssss* refers to two hexads, AcORSRSRSOMe and AcOSRSRSROMe. In this thesis, the methine carbon atoms in each *n*-ad are numbered from left to right, with 1 corresponding to the methine next to the acetate ester.

Characterization of the methine region (68.0-69.5 ppm) of the ^{13}C-NMR spectra was emphasized since prior work on poly(lactide) focused on assigning these resonances. Less useful was the methyl region, which often contains overlapping peaks, and the carbonyl region, which could not be successfully analyzed in each case due to low signal-to-noise ratios. Each hexad had six methine resonances in the ^{13}C-NMR. The corresponding methine region in the ^{1}H-NMR was a complex multiplet from overlapping quartets, and could not be successfully decoupled.

Table 2.2. Hexads Synthesized.

Tacticity	Hexad	Tacticity	Hexad
sssis	SRSRRS	*isiii*	RRSSSS
iiiis	RRRRRS	*sssii*	RSRSSS
iisss	RRRSRS	*ssiis*	RSRRRS
iiiss	SSSSRS	*issii*	SSRSSS
ssiii	SRSSSS	*iissi*	SSSRSS
isiss	RRSSRS	*sisis*	RSSRRS
isisi	SSRRSS	*issis*	RRSRRS
isssi	RRSRSS	*sssss*	RSRSRS
iiiii	SSSSSS		

Each hexad has a characteristic ^{13}C-NMR signature in terms of the placement of the methine resonances. By considering the trends seen in the hexads as well as data from shorter *n*-ads, each methine resonance was assigned as outlined below. In the spectra of the *is* diad and the structurally related *iis* triad (Figure 2.2), the most downfield and upfield peaks in each spectrum have similar chemical shifts. The first and last methine in each *n*-ad are in similar chemical environments, resulting in the methine assignments shown in Figure 2.2. Analogous trends are observed for the *iii*, *iiii*, and *iiiii* *n*-ads (Figure 2.3), where a comparison of the spectra show that each resonance in the

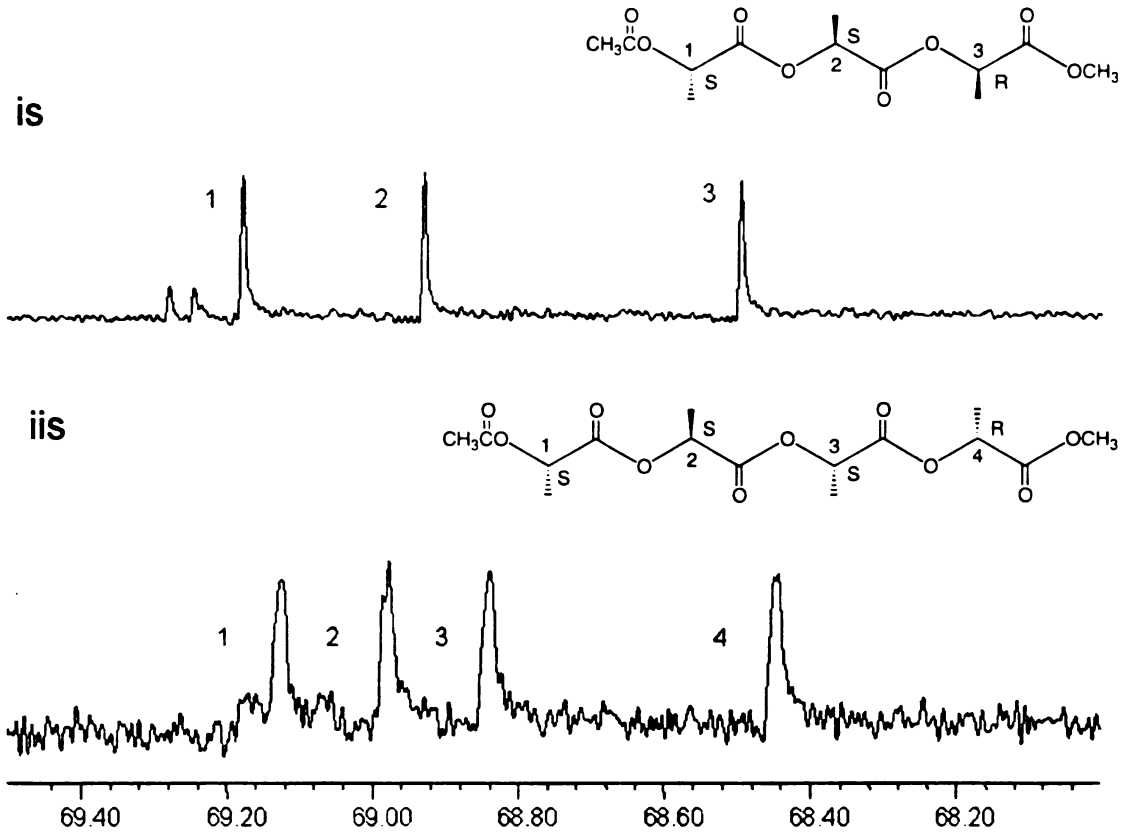

Figure 2.2. Comparison of methine regions of *is* and *iis* *n*-ads

shorter *n*-ad has a analogous resonance in the longer *n*-ad with a similar chemical shift. The first three methines in each *n*-ad have similar chemical shifts and hence similar chemical environments. The most downfield resonance in each was assigned to the methine adjacent to the acetate, while the most upfield resonance was assigned to the methine adjacent to the methyl ester because of the similarity of the chemical shift to the most upfield resonance in most *n*-ads that have an isotactic stereochemical relationship between the first two centers. With the most upfield and downfield chemical shifts assigned, the peaks due to methines 2 and 3 remain to be assigned in the *iii* tetrad. These resonances correspond to methines 2 and 3, and were assigned on the basis of their distance from the acetate and methyl ester.

The *iiii* pentad requires assignment of one additional resonance. A comparison of the *iii* and *iiii* methine regions shows that the first three resonances map onto one another. Assuming the assignment of these three peaks are the same in each member of the series and assigning the most upfield resonance as the methine nearest the methyl ester, the peak at 68.80 ppm was assigned as methine 4. Following the same pattern, five out of the six peaks in the ^{13}C NMR of the *iiiii* hexad (Figure 2.3) were assigned, and the new peak was identified as methine 5.

The methine regions of the remaining hexads were assigned using the same approach, a comparison of the ^{13}C NMR spectra with those of hexads that share some of the same stereochemical sequences. For example, a comparison of the methine region in the ^{13}C NMR spectra of the *iiiii* and the *iiiis* hexads (Figure 2.4) shows that they differ only in the position of the most upfield resonance. Since the difference between the two hexads is stereochemistry of the methine nearest the methyl ester, the peak at 68.49 ppm in the spectrum of the *iiiis* hexad is methine 6.

Similar logic was used to assign the methine region of the *isiii* hexad (Figure 2.5). Assignment of the *isisi* hexad follows from a comparison of the *isisi* spectrum with that of the *isiii* hexad, which shows that resonances 4 and 5 of the *isisi* hexad are shifted downfield relative to methines 4 and 5 of the *isiii* hexad. The effect of the syndiotactic dyad can be more clearly seen if the spectra of *isiss* and *isisi* are compared. The most downfield methine peak of the *isiss* hexad is shifted quite drastically downfield compared to that of the *isisi* methine region.

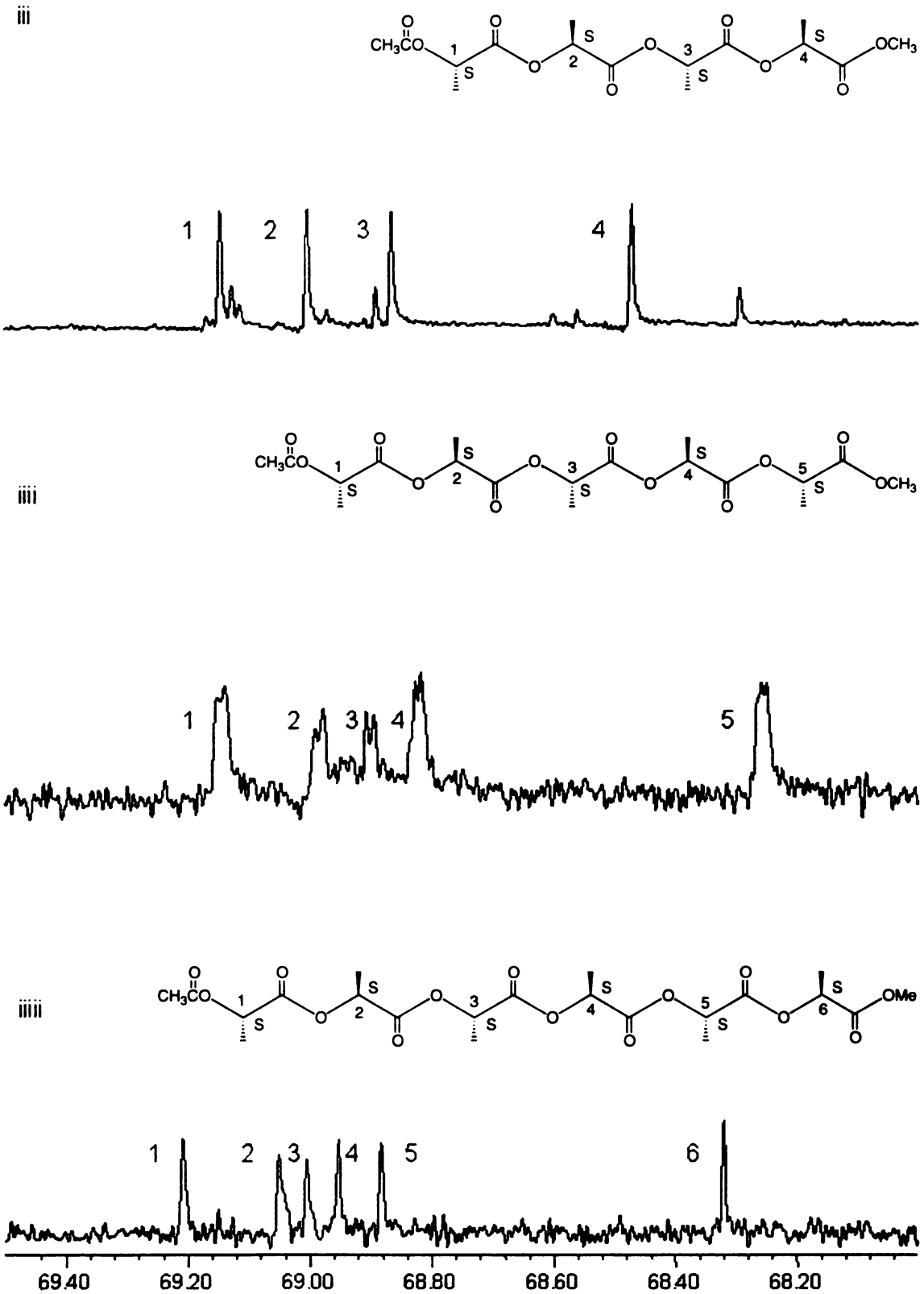

Figure 2.3. Comparison of the methine regions of the *iii*, *iiii*, *iiiii* *n*-ads.

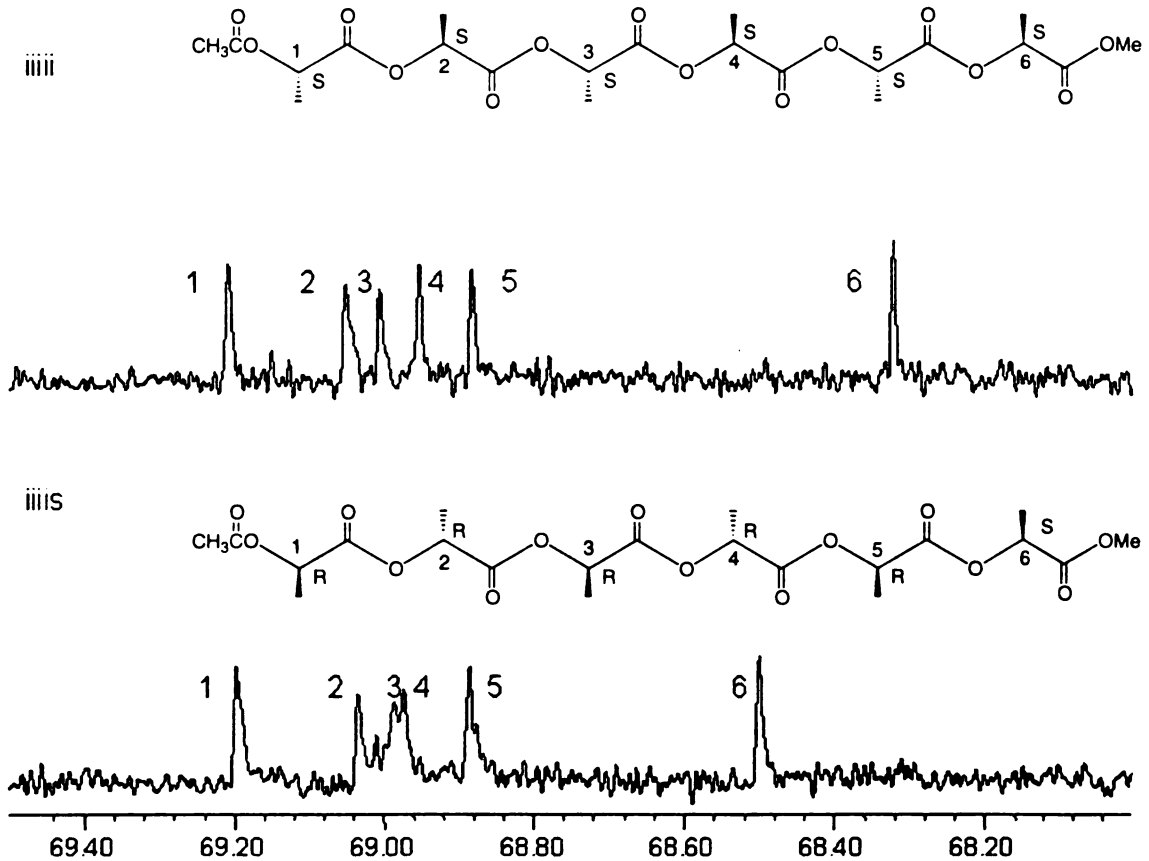

Figure 2.4. Comparison of the methine regions of the *iiiii* and *iiiis* hexads.

The remaining peaks of the *isiss* methine region can be assigned by comparison to the methine region of the *isisi* hexad; the most downfield peak was assigned as methine 5 (Figure 2.5).

The effect of syndiotactic dyads on the chemical shift of the methines can be most clearly seen when one compares the methine regions of the *ssiii*, *sssii*, and *sssss* spectra (Figure 2.6). As more adjoining syndiotactic dyads are added, the resonances shift downfield. If we consider a polylactide chain in a planar zigzag conformation, a syndiotactic relationship between two adjoining stereocenters places the methyl groups on the same side of the plane defined by

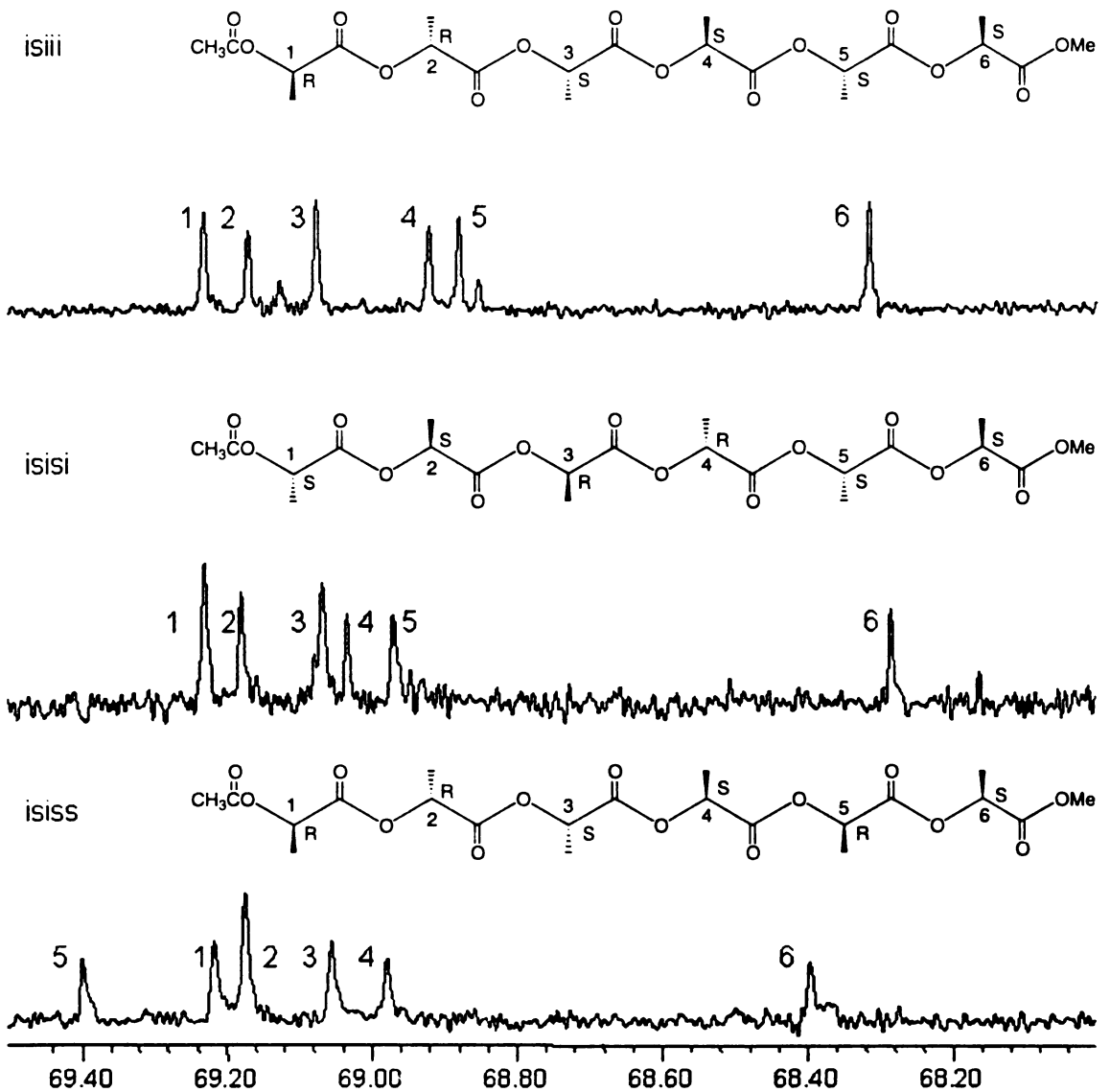

Figure 2.5. Comparison of the *isiii, isisi, isiss* hexad methine regions.

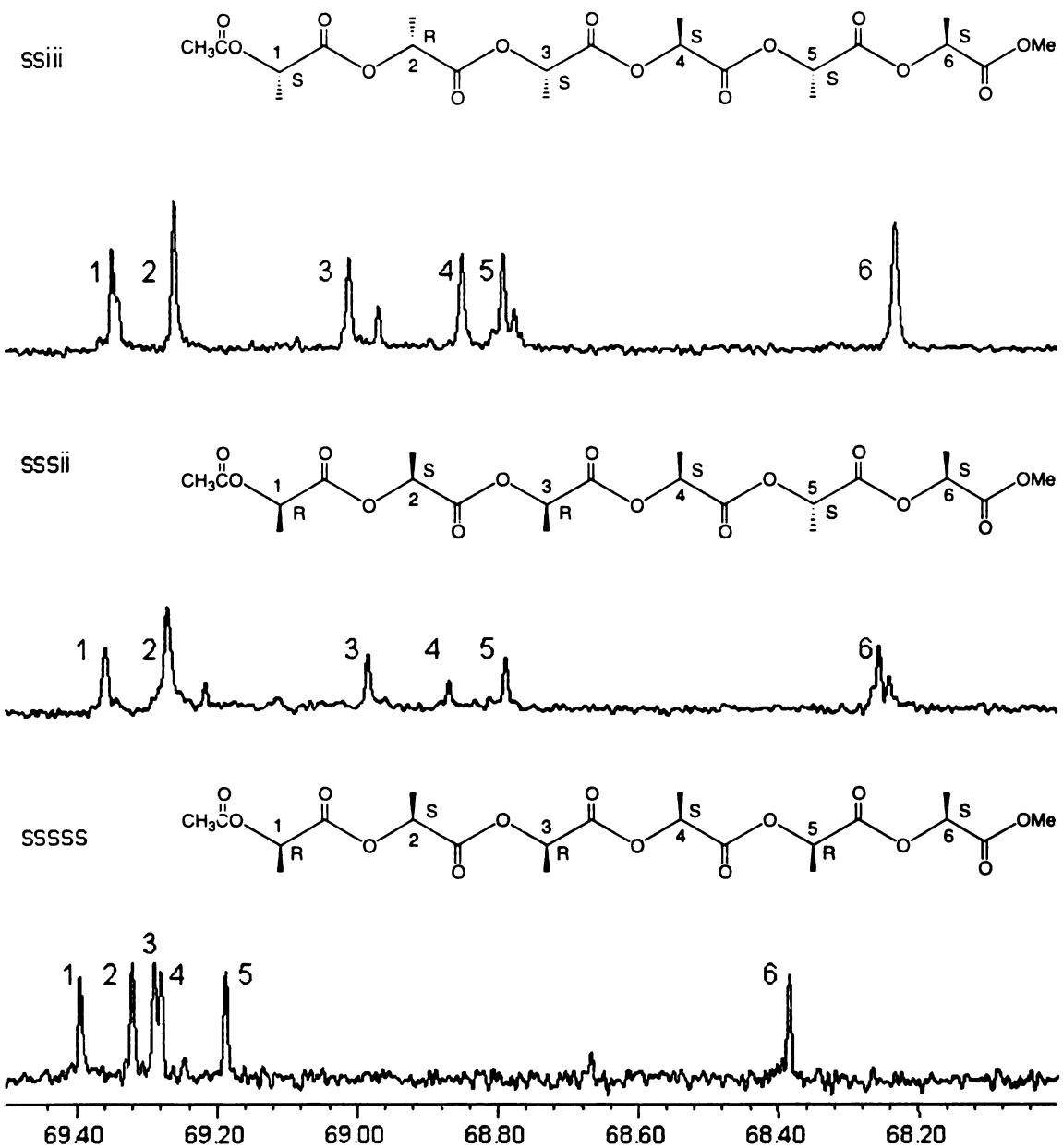

Figure 2.6. Comparison of the methine regions of *ssiii*, *sssii*, *sssss* hexads.

the polymer backbone, deshielding the methine carbon and shifting the methine resonance downfield relative to an isotactic dyad. Using the methods outlined above, the methine region of the ^{13}C NMR of each hexad was assigned. The results are summarized in Table 2.3.

A simple model was devised to test for consistency in the assignment of the chemical shifts. The approach is similar to the models developed for the prediction of the chemical shifts in polypropylene and polypropylene oxide. For a given resonance, the effects of adjacent stereocenters (α relationship), as well as next nearest neighbors (β relationship) are considered. A γ effect, similar to the γ relationship in poly(propylene) and poly(propylene oxide) could also be included. Using the *iiiii* hexad as the reference, the chemical shift of a methine in a given stereosequence is calculated by adding corrective factors to the base chemical shift for the methine of interest. For example, the chemical shift of methine 3 of the *isiii* hexad (Figure 2.7) is calculated by adding corrective factors to the methine chemical shift of the third methine from the *iiiii* hexad (Eq. 2.1).

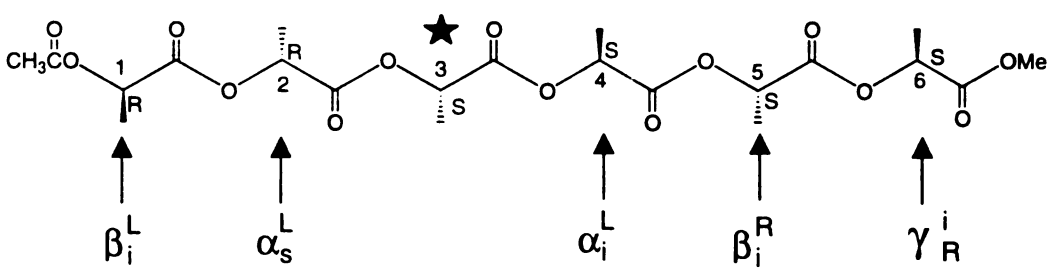

Figure 2.7. *isiii* hexad.

Methine 3 chemical shift=*iiiii* base + $\alpha^L{}_s + \alpha^R{}_i + \beta^L{}_i + \beta^R{}_i + \gamma^R{}_i$ Eq. 2.1

Table 2.3. Summary of Hexad Methine Shifts.

Sequence	1	2	3	4	5	6
iiiii	69.21	69.05	69.00	68.95	68.88	68.33
isiii	69.22	69.16	69.07	68.91	68.87	68.30
isiss	69.21	69.17	69.05	68.97	69.39	68.39
isisi	69.23	69.18	69.07	69.04	68.97	68.28
issis	69.23	69.10	69.42	69.05	68.89	68.52
issii	69.21	69.08	69.41	69.02	68.84	68.29
iiiis	69.19	69.03	68.98	68.97	68.88	68.49
iissi	69.19	69.05	68.93	69.37	69.03	68.30
iisss	69.19	69.04	69.01	69.39	69.18	68.39
isssi	69.22	69.07	69.40	69.28	69.18	68.38
iiiss	69.20	69.02	69.01	69.00	69.29	68.39
sssss	69.39	69.32	69.28	69.27	69.18	68.38
ssiis	69.36	69.27	69.01	68.91	68.82	68.44
ssiii	69.34	69.26	69.01	68.85	68.79	68.24
sssii	69.36	69.27	68.98	68.87	68.79	68.26
sisis	69.30	69.14	69.14	68.98	68.85	68.48
sssis	69.31	69.23	69.23	68.96	68.78	68.41

The corrective factors were estimated by using a broad range of values for the corrective factors to calculate the chemical shifts of each methine in each hexad. An Excel spreadsheet was used to compare the calculated and experimentally measured values, and the sum of the squares of the deviations (observed – calculated)^2 was used to test for the quality of fit. The corrective factors values that gave the minimum sum of the squares of the deviations are summarized in Table 2.4. The calculated shifts are found in Table 2.5.

Table 2.4. Corrective factors

α^L_s	α^L_i	α^R_s	α^R_i
0.06	-0.12	0.19	0.02
β^L_i	β^L_s	β^R_i	β^R_s
0.01	-0.03	0.00	-0.03
γ^R_i	γ^R_s	γ^L_i	γ^L_s
0.07	0.05	0.00	0.06

In general, the calculated chemical shifts match the experimental values reasonably well. However, hexads with *ss* sequences often show substantial deviation and either the assignments of these hexads are incorrect or considering only adjacent and next nearest neighbor interactions is inadequate.

In principle, NMR experiments could be used to confirm the assignment of the methine carbons. If the acetate or the methyl ester carbons could be selectively excited, the transfer of excitation to the neighboring methine would

Table 2.5. Calculated Methine ^{13}C Chemical Shifts

	Methine Carbon in Hexad					
Hexad	1	2	3	4	5	6
iiiii	69.21	69.05	69.00	68.95	68.88	68.33
isiii	69.20	69.12	69.09	68.89	68.84	68.29
isiss	69.20	69.18	69.12	69.03	69.19	68.43
isisi	69.20	69.18	69.06	69.06	69.02	68.25
issis	69.26	69.09	69.32	69.04	68.97	68.45
issii	69.26	69.09	69.26	69.07	68.80	68.27
iiiis	69.23	68.95	68.97	68.90	69.03	68.47
iissi	69.29	68.98	69.05	69.28	69.00	68.23
iisss	69.29	68.98	69.11	69.25	69.17	68.41
isssi	69.26	69.15	69.23	69.24	68.98	68.23
iiiss	69.23	69.01	68.94	69.07	69.21	68.43
sssss	69.43	69.33	69.25	69.19	69.15	68.41
ssiis	69.37	69.30	69.11	68.84	69.01	68.47
ssiii	69.37	69.30	69.05	68.87	68.84	68.29
sssii	69.43	69.27	69.22	69.05	68.80	68.27
sisis	69.43	69.10	69.10	69.06	68.99	68.45
sssis	69.43	69.27	69.28	69.02	68.98	68.45

Table 2.6. Deviations in Calculation of Chemical Shift of Hexads.

	Methine Carbon in Hexad					
Hexad	1	2	3	4	5	6
iiiii	0.00	0.00	0.00	0.00	0.00	0.00
isiii	0.02	0.04	-0.03	0.02	0.03	0.02
isiss	0.01	-0.01	-0.07	-0.06	0.20	-0.03
isisi	0.03	0.00	0.00	-0.03	-0.06	0.04
issis	-0.03	0.01	0.10	0.01	-0.08	0.07
issii	-0.05	-0.01	0.14	-0.05	0.03	0.02
iiiis	-0.04	0.08	0.01	0.07	-0.15	0.03
iissi	-0.10	0.07	-0.13	0.09	0.03	0.08
iisss	-0.10	0.06	-0.10	0.14	0.01	-0.02
isssi	-0.04	-0.09	0.17	0.04	0.20	0.15
iiiss	0.03	-0.01	-0.06	0.07	-0.08	0.04
sssss	0.04	0.01	-0.03	-0.08	-0.03	0.03
ssiis	-0.01	-0.03	-0.11	0.07	-0.20	-0.02
ssiii	-0.03	-0.04	-0.05	-0.02	-0.05	-0.05
sssii	-0.07	0.00	-0.24	-0.18	-0.01	-0.01
sisis	-0.13	0.04	0.03	-0.08	-0.14	0.03
sssis	-0.12	-0.04	-0.05	-0.06	-0.20	-0.04
deviation		*0.03*	*0.17*	*0.10*	*0.18*	

reveal the connectivity in the hexad. Repeating the process would allow "sequencing" of the hexad. The HMBC (heteronuclear multiple bond correlation) experiment is a two-dimensional experiment which reveals long range coupling

between carbons and hydrogens. It was hoped that the acetate methyl group would correlate with the nearest methine carbon or hydrogen. However the coupling was not strong enough to result in a cross peak (Figure 2.8, 2.9).

A NOE (Nuclear Overhauser Effect) experiment also was ineffective. It was thought that through-space interactions may lead to a more conclusive assignment of the methines. However the only correlation detected was between the methyl and the methine hydrogens. A small NOE effect between the methyl group of the ester and the acetate methyl group suggested a hairpin conformation for the hexad. Preliminary molecular modeling showed that the hairpin shape was plausible since it corresponded to one of the lowest energy conformations of the hexad.

Several other two-dimensional experiments were tried. NOESY (Nuclear Overhauser Effect Spectroscopy) is a two-dimensional experiment in which direct, through space dipole-dipole interactions can been seen. This experiment confirmed the one-dimensional NOE findings, but was not helpful in assigning the resonances since there were no cross peaks were observed.

The cross-peaks in the 2D spectrum of an HMQC (Heteronuclear Multiple-Quantum Coherence) experiment arise from the protons directly bonded to ^{13}C atoms. The HMQC (Figures 2.10 and 2.11) spectrum confirmed that the methyl hydrogens were directly connected to the methyl carbons. It also confirmed that the methine hydrogens were directly connected to the methine carbons. No long range coupling between hydrogens and carbons was observed.

Several T_1 experiments were also tried. It was thought that if the acetate group could be selectively excited, the relaxation time for the nearest methine carbon would be longer than that of a more distant methine carbon. However, the T_1 times of the methine carbons were too similar to be assigned conclusively.

In conclusion, by comparing various polylactide hexads and smaller oligomers, a mathematical relationship was devised to further understand the stereochemical relationships in polylactide. The "discrepancy" found in the HETCOR spectrum as described by Chisholm[3] is probably due to chemical tensor effects, since the chemical shift can be predicted to some degree of certainty. Further progress in this area will likely require the use of isotopically labeled hexads to enable a more conclusive assignment of the resonances. Molecular modeling may also provide a better understanding of the stereochemically dependent conformation of hexads and its impact, if any, on the chemical shift of the methines. Since the conformation of a hexad in a "good" solvent the hexad should be linear, but bent in a "bad" solvent, solvent effects may affect the chemical shift of the methine carbons and play a role in the outcome of the NOE experiments.

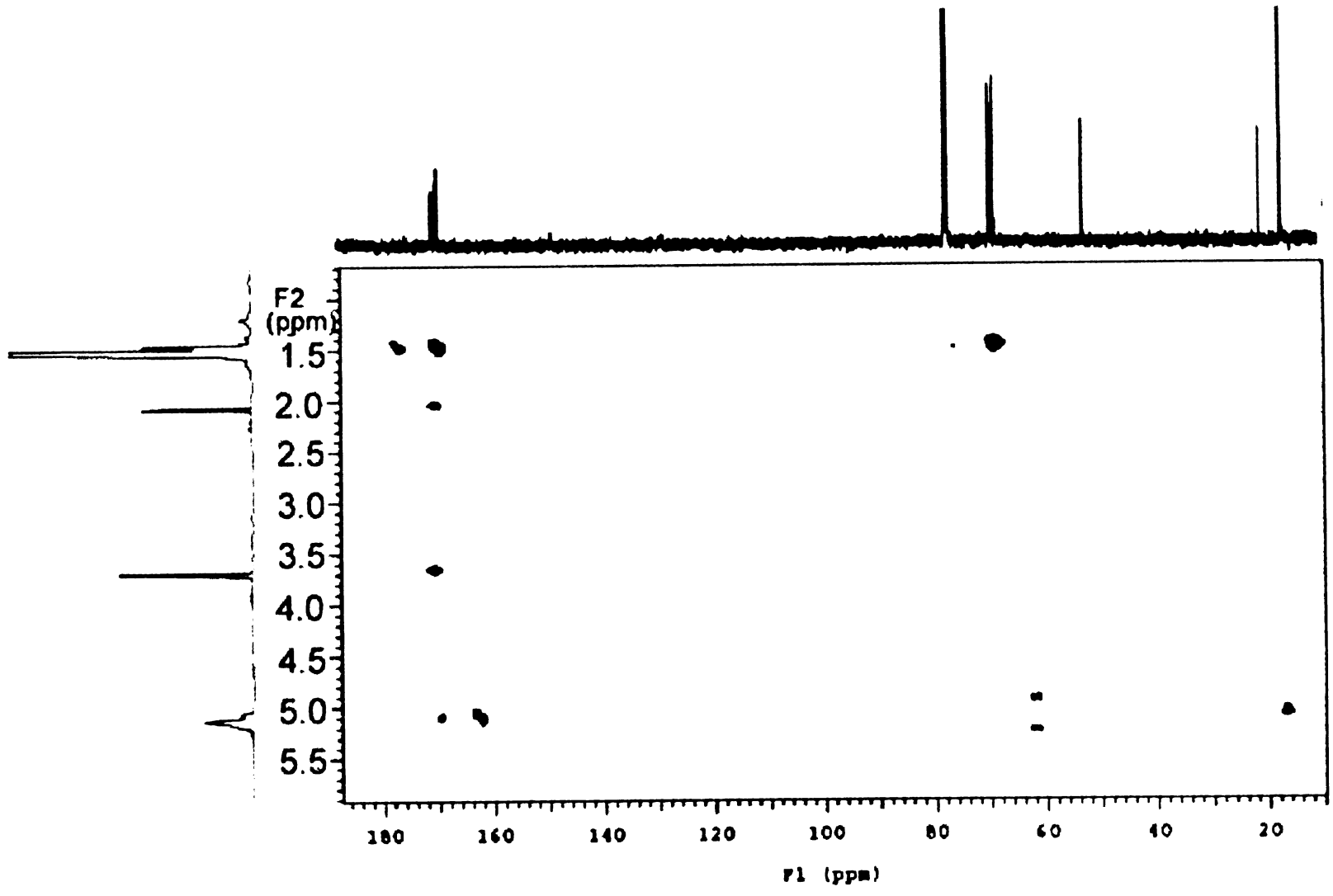

Figure 2.8. HMBC of *iissi* hexad.

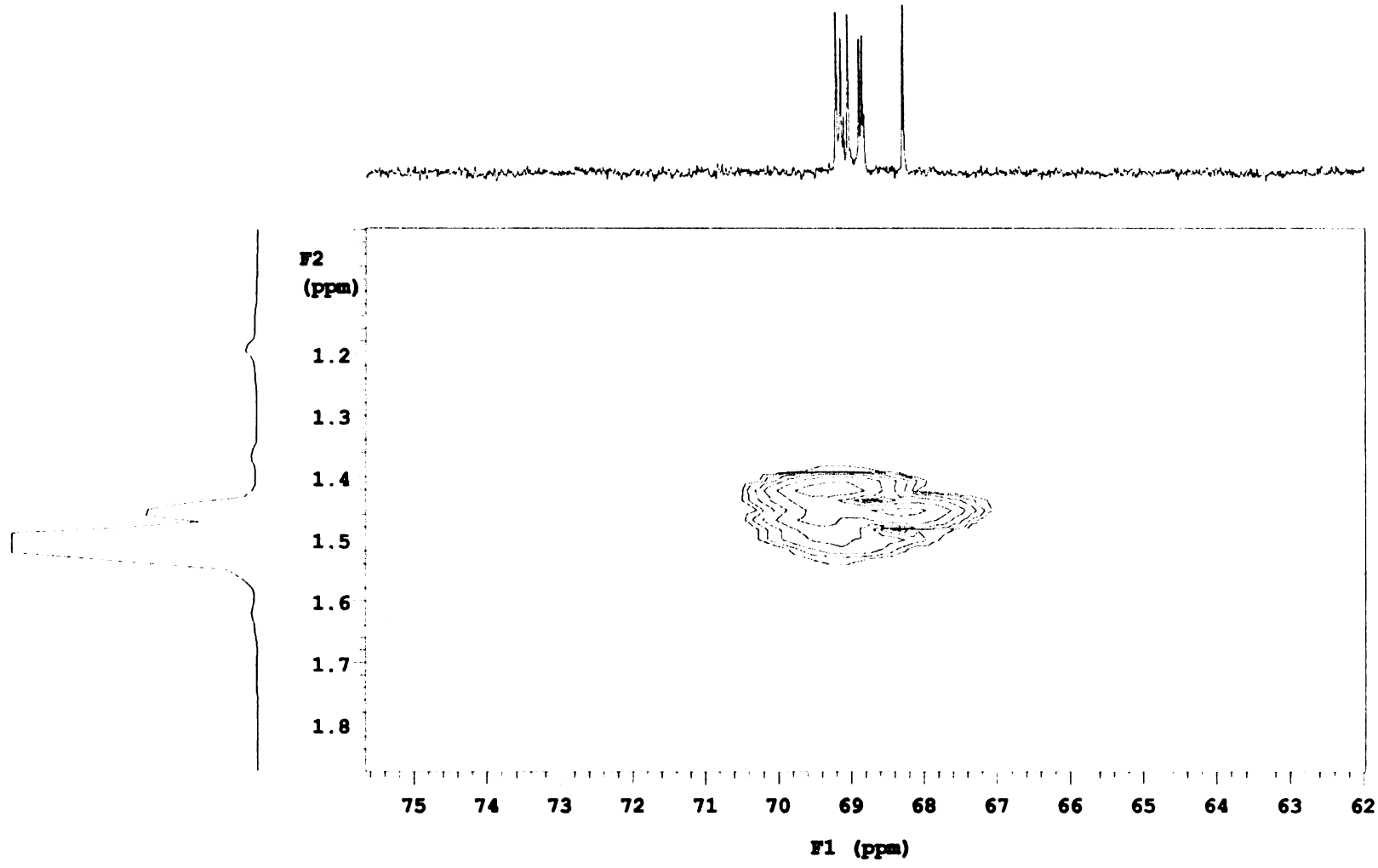

Figure 2.9. Expansion of *iissi* hexad HMBC.

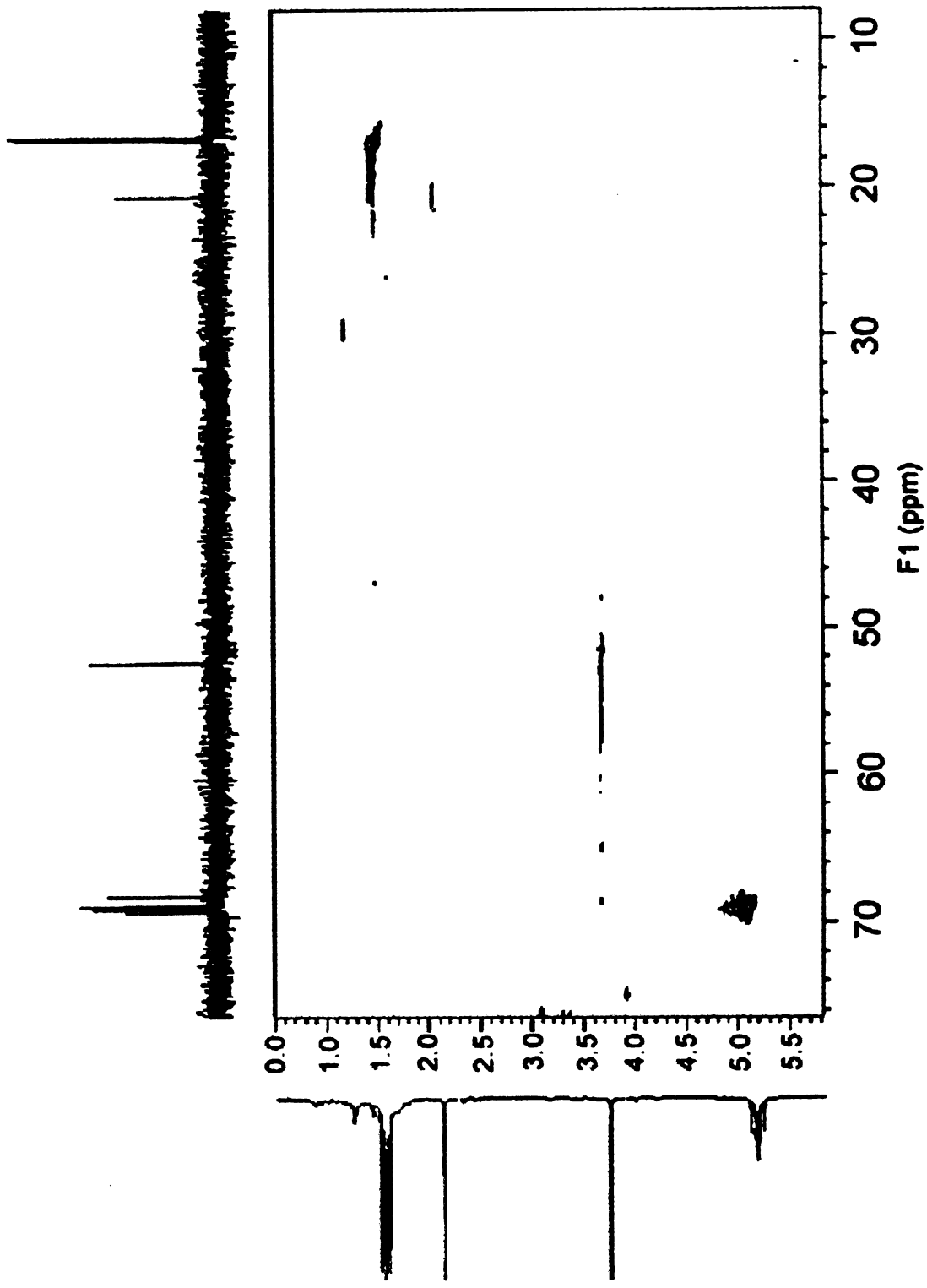

Figure 2.10. HMQC of *iissi* hexad.

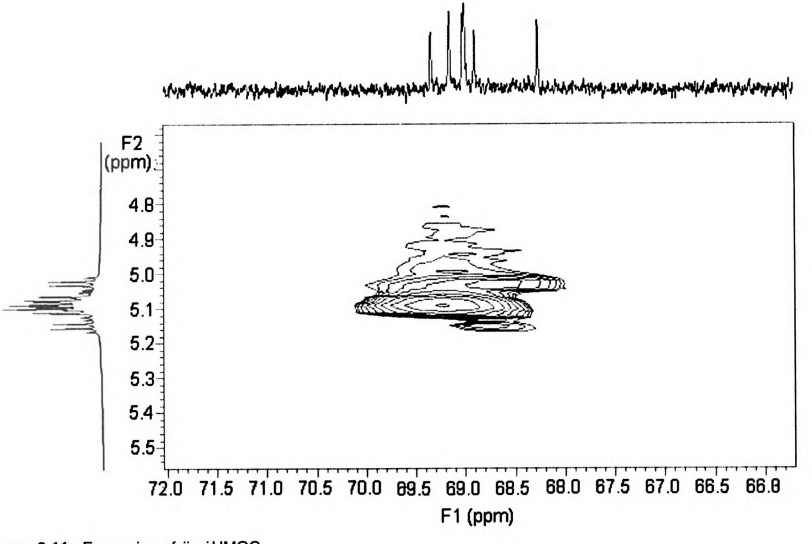

Figure 2.11. Expansion of *iissi* HMQC.

2.1 References

1. Kricheldorf, H. R.; Boettcher, C.; Tonnes, K.-U. *Polymer* **1992**, *33*, 2817-2824.

2. Thakur, K. A. M.; Kean, R. T.; Hall, E. S.; Kolstad, J. J.; Lindgren, T. A. *Macromolecules* **1997**, *30*, 2422-2428.

3. Chisholm, M. H.; Iyer, S. S.; Matison, M. E.; McCollum, D. G.; Pagel, M. *Chemical Communications* **1997**, 1999-2000.

3. Experimental

General. CH_2Cl_2 was distilled over CaH_2 prior to use. Pd/C was stored in a helium-filled dry box. L-lactide was obtained from Aldrich and D-Lactide from Purac. Both lactides were purified by recrystalization from ethyl acetate. All other chemicals and solvents were used as received. All hexad ^{13}C NMR spectra were obtained on a Varian 500 MHz spectrometer as 15 wt% solutions in $CDCl_3$.

Abbreviations for compounds. For convenience, each hexad is symbolically represented to reflect the stereochemistry of each lactic acid residue with the end groups denoted by standard abbreviations. Thus, (2R)-2-{{(2'S)-2'-{{(2"R)-2"-{{(2"'S)-2"'-{{(2""S)-2""{{(2"""S)-2"""-benzyloxypropanoyl}oxy} propanoyl}oxy}propanoyl}oxy}propanoyl}oxy}propanoyl}oxy}propanoic acid methyl ester is represented as BnORSRSSSOMe. Similarly, its acetylated derivative is abbreviated as AcORSRSSSOMe rather than (R,S,R,S,S,S)-α-acetyl-ϕ-(methoxy)hexakis[oxy(1-methyl-2-oxoethane-1,2-diyl)]. Compounds that have a hydroxy terminus such as (2S)-2-{{(2'S)-2'-{{(2"S)-2"-{{(2"'R)-2"'-{{(2""S-2""-hydroxypropanoyl}oxy}propanoyl}oxy}propanoyl}oxy}propanoyl}oxy} propanoic acid methyl ester are abbreviated as HOSSSRSOMe.

(S)-2-Benzyloxypropanoic acid, methyl ester. (*S*)-2-Hydroxypropanoic acid ethyl ester (16.43 g, 9.08 mmol) and benzyl bromide (5.00 g, 4.59 mmol) were added to a stirred solution of Ag(I)O (11.135 g, 4.59 mmol) in 25 mL of dry CH_2Cl_2. After stirring at room temperature for 24 hours, the reaction mixture was filtered and the solvent was removed via rotary evaporation. The crude product

was not purified further. ^{1}H NMR (300 MHz, $CDCl_3$): δ 7.28 (m, 5H), 4.57 (d, 2H), 4.08 (q, 1H), 3.72 (s, 3H), 1.43 (d, 3H)

(R)-2-Benzyloxypropanoic acid, methyl ester. Prepared as described above, except (*R*)-2-hydroxypropanoic acid methyl ester was used as the starting material. ^{1}H NMR (300 MHz, $CDCl_3$): δ 7.28 (m, 5H), 4.57 (d, 2H), 4.08 (q, 1H), 3.72 (s, 3H), 1.43 (d, 3H)

(R)-2-Benzyloxypropanoic acid, isobutyl ester. Prepared as described above, except (*R*)-2-hydroxypropanoic acid isobutyl ester was used as the starting material. ^{1}H NMR (300 MHz, $CDCl_3$): δ 7.31 (m, 5H), 4.53 (dd, 2H), 4.08 (q, 1H), 3.97 (m, 2H), 1.95 (septuplet, 1H), 1.41 (d, 3H), 0.91 (d, 6H)

(S)-2-Benzyloxylpropanoic acid. (S)-2-Benzyloxylpropanoic acid methyl ester 13.21 g (0.0634 moles) was added to a mixture of 300 mL of 0.2 M aqueous LiOH and 300 mL of THF. After stirring at room temperature for 5 days, most of the THF was removed via rotary evaporation. The resulting aqueous mixture was extracted with ether (3 x 100 mL), and then the combined organic layers were washed with sat. $NaHCO_3$ (3 x 75 mL). The aqueous layers were combined and acidified to pH 1 with conc. HCl, and were then extracted with ether (3 × 100 mL). The organic layers were dried over $MgSO_4$, filtered, and concentrated by rotary evaporation to give 10.21 g (89%) of a white solid. ^{1}H NMR (300 MHz, $CDCl_3$): δ 9.28 (br s, 1H), 7.31 (m, 5H), 4.80 (dd, 2H), 4.11 (q, 1H), 1.50 (d, 3H)

(R)-2-Benzyloxylpropanoic Acid. Prepared as described above except (*R*)-2-hydroxypropanoic acid methyl ester was used as the starting material. ^{1}H

NMR (300 MHz, $CDCl_3$): δ 9.28 (br s, 1H), 7.31 (m, 5H), 4.80 (dd, 2H), 4.11 (q, 1H), 1.50 (d, 3H)

HOSOMe. A mixture of L-Lactide 5.50 g (0.0382 moles) and 10 mL of conc. HCl in 800 mL of methanol was heated to the reflux temperature for 24 hours. The solution was cooled, and all methanol was removed by rotary evaporation to give 3.92 g of the ester (0.0400 mol, 49%) as a clear colorless oil. NMR spectroscopy showed that the product was pure. ^1H NMR (300 MHz, $CDCl_3$): δ 9.28 (s, 1H), 7.18 (m, 5H), 4.60 (dd, 2H), 4.09 (q, 1H), 1.51 (d, 3H)

HOROMe. Prepared as described above except 50.0 g (0.347 moles) D-Lactide was used as the starting material. Yield: 63.15 g of the ester (0.61 mol, 88%) as a clear colorless oil. NMR spectroscopy showed that the product was pure. ^1H NMR (300 MHz, $CDCl_3$): δ 9.0 (s, 1H), 7.30 (m, 5H), 4.60 (dd, 2H), 4.11 (q, 1H), 1.45 (t, 3H)

HOSSOMe. L-Lactide 24.55 g (0. 170 moles) in 500 mL of methanol was heated to the reflux temperature for 24 hours. The solution was cooled, and all methanol was removed by rotary evaporation to give 27.22 g of the ester (0.15 moles, 91%) as a clear colorless oil. NMR spectroscopy showed that the product was pure. ^1H NMR (300 MHz, $CDCl_3$): δ 5.13 (m, 2H), 4.30 (q, 1H), 3.72 (s, 3H), 2.85 (s br, 1H), 1.58 (d, 3H), 1.44 (m, 6H)

Hydrogenation. All hydrogenation reactions were carried out using the same procedure. To a Parr bomb fitted with a glass sleeve and a stir bar, 5 mL of diethyl ether was added to 0.0615 g (0.1186 mmol) BnORRSRSOMe. 0.06 g of 10% Pd/C was added, the bomb was purged three times with N_2, and then filled

with H_2 (1200 psi). The reaction was monitored by NMR. Upon completion of the reaction, the heterogeneous mixture was gravity filtered to remove Pd/C, and removal of the ether gave a clear, colorless liquid in 87% yield (0.05033g). NMR data for the hydroxy terminated compounds appear in Tables 3.1-3.5.

Coupling Procedure with (R)- or (S)-Benzyloxylpropanoic acid. (S)-2-Benzyloxylpropanoic acid (0.0160 g, 0.0885 mmol), HORRRSOMe (0.0313 g, 0.0737 mmol), EDC (0.212 g, 0.1106 mmol), DMAP (0.0018 g, 0.0147 mmol), and 2 mL of dry CH_2Cl_2 were added to a round bottom flask at room temperature. After stirring for a half hour, the solution was washed with 0.5 M HCl (3 x 5 mL), followed by 5 mL of sat. $NaHCO_3$. The organic layer was dried over $MgSO_4$. Following filtration, the solvent was removed via rotary evaporation to give 0.0299g (0.0510mmol, 69%) of a clear, colorless liquid. The product was determined to be pure by NMR. NMR data for benzyl terminated compounds appear in Tables 3.6-3.10.

Coupling Procedure with Acetic Acid. Acetic acid (0.282 g, 0.4694 mmol), HORSSSOMe (0.1000 g, 0.3139 mmol), EDC (0.0902 g, 0.4709 mmol), DMAP (0.0077g, 0.0630 mmol), and 2 mL of dry CH_2Cl_2 were added to a round bottom flask at room temperature. After stirring for a half hour, the solution was washed with 0.5 M HCl (3 x 5 mL) followed by 5 mL of sat. $NaHCO_3$. The organic layer was dried over $MgSO_4$. Following filtration, the solvent was removed via rotary evaporation to yield 0.0736 g (0.0204 mmol, 65%) of a clear, colorless liquid. The product was determined to be pure by NMR. NMR data for the benzyl terminated compounds appear in Tables 3.11-3.14.

Table 3.1. Yield and ^{1}H-NMR Data for Hydroxy-terminated Diad

Compound	% Yield	^{1}H NMR (300 MHz, $CDCl_3$)
HORSOMe	83%	5.18 (q, 1H), 4.38 (q, 1H), 3.75 (s, 3H), 3.17 (br s, 1H), 1.49 (d, 3H), 1.40 (d, 3H)

Table 3.2. Yields and ^{1}H-NMR Data for Hydroxy-terminated Triads

Compound	% Yield	^{1}H NMR (300 MHz, $CDCl_3$)
HOSSSOMe	87%	5.20 (m, 2H), 4.37 (q, 1H), 3.73 (s, 3H), 2.69 (br s, 1H), 1.57 (d, 3H), 1.48 (m, 6H)
HORSSOMe	82%	5.20 (m, 2H), 4.37 (q, 1H), 3.73 (s, 3H), 2.69 (br s, 1H), 1.57 (d, 3H), 1.48 (m, 6H)
HORRSOMe	50%	5.20 (m, 2H), 4.37 (q, 1H), 3.73 (s, 3H), 2.69 (br s, 1H), 1.57 (d, 3H), 1.48 (m, 6H)
HOSRSOMe	69%	5.20 (m, 2H), 4.37 (q, 1H), 3.73 (s, 3H), 2.69 (br s, 1H), 1.57 (d, 3H), 1.48 (m, 6H)

Table 3.3. Yields and ^{1}H-NMR Data for Hydroxy-terminated Tetrads

Compound	% Yield	^{1}H NMR (300 MHz, $CDCl_3$)
HORSRSOMe	87%	5.18 (m, 3H), 4.39 (q, 1H), 3.71(s, 3H), 1.50 (m, 12H)
HOSSRSOMe	92%	5.18 (m, 3H), 4.39 (q, 1H), 3.71(s, 3H), 1.50 (m, 12H)
HOSRRSOMe	97%	5.18 (m, 3H), 4.39 (q, 1H), 3.71(s, 3H), 1.50 (m, 12H)
HORSSSOMe	88%	5.17 (m, 5H), 4.32 (q, 1H), 3.71 (s, 3H), 1.43 (m, 12H)
HOSSSSOMe	90%	5.17 (m, 5H), 4.32 (q, 1H), 3.71 (s, 3H), 1.43 (m, 12H)
HORRSSOMe	97%	5.17 (m, 5H), 4.32 (q, 1H), 3.71 (s, 3H), 1.43 (m, 12H)
HOSRSSOMe	76%	5.17 (m, 5H), 4.32 (q, 1H), 3.71 (s, 3H), 1.43 (m, 12H)
HORRRSOMe	88%	5.17 (m, 5H), 4.32 (q, 1H), 3.71 (s, 3H), 1.43 (m, 12H)
HOSRRSOMe	91%	5.17 (m, 5H), 4.32 (q, 1H), 3.71 (s, 3H), 1.43 (m, 12H)
HORSRSOMe	68%	5.17 (m, 5H), 4.32 (q, 1H), 3.71 (s, 3H), 1.43 (m, 12H)
HORSSSOMe	78%	5.17 (m, 5H), 4.32 (q, 1H), 3.71 (s, 3H), 1.43 (m, 12H)
HOSSRSOMe	82%	5.17 (m, 5H), 4.32 (q, 1H), 3.71 (s, 3H), 1.43 (m, 12H)

Table 3.4. Yields and ^{1}H-NMR Data for Hydroxy-terminated Pentads

Compound	% Yield	^{1}H NMR (300 MHz, $CDCl_3$)
HORSSRSOMe	78%	5.18 (m, 4H), 4.39(q, 1H), 3.72 (s, 3H), 1.48 (m, 15H)
HOSSSSSOMe	82%	5.18 (m, 4H), 4.39(q, 1H), 3.72 (s, 3H), 1.48 (m, 15H)
HOSSRRSOMe	56%	5.18 (m, 4H), 4.39(q, 1H), 3.72 (s, 3H), 1.48 (m, 15H)
HORSSSSOMe	65%	5.18 (m, 4H), 4.39(q, 1H), 3.72 (s, 3H), 1.48 (m, 15H)
HOSRSSSOMe	82%	5.18 (m, 4H), 4.39(q, 1H), 3.72 (s, 3H), 1.48 (m, 15H)
HOSSSSSOMe	40%	5.18 (m, 4H), 4.39(q, 1H), 3.72 (s, 3H), 1.48 (m, 15H)
HORRRSSOMe	92%	5.18 (m, 4H), 4.39(q, 1H), 3.72 (s, 3H), 1.48 (m, 15H)
HOSRRSSOMe	99%	5.18 (m, 4H), 4.39(q, 1H), 3.72 (s, 3H), 1.48 (m, 15H)
HORSRSSOMe	36%	5.18 (m, 4H), 4.39(q, 1H), 3.72 (s, 3H), 1.48 (m, 15H)
HORRRSSOMe	87%	5.18 (m, 4H), 4.39(q, 1H), 3.72 (s, 3H), 1.48 (m, 15H)
HOSSRSSOMe	84%	5.18 (m, 4H), 4.39(q, 1H), 3.72 (s, 3H), 1.48 (m, 15H)
HORRSSSOMe	94%	5.18 (m, 4H), 4.39(q, 1H), 3.72 (s, 3H), 1.48 (m, 15H)
HOSRRRSOMe	95%	5.18 (m, 4H), 4.39(q, 1H), 3.72 (s, 3H), 1.48 (m, 15H)
HORRSRSOMe	87%	5.18 (m, 4H), 4.39(q, 1H), 3.72 (s, 3H), 1.48 (m, 15H)

Table 3.4. (cont'd).

HOSRSRSOMe	87%	5.18 (m, 4H), 4.39(q, 1H), 3.72 (s, 3H), 1.48 (m, 15H)
HOSRSSSOMe	47%	5.18 (m, 5H), 4.39(q, 1H), 3.72 (s, 3H), 1.48 (m, 18H)

Table 3.5. Yields and ^{1}H-NMR Data for Hydroxy-terminated Hexads

Compound	% Yield	^{1}H NMR (300 MHz, $CDCl_3$)
HOSSSSSSOMe	57%	5.18 (m, 4H), 4.39(q, 1H), 3.72 (s, 3H), 1.48 (m, 15H)
HOSSRSSSOMe	78%	5.18 (m, 4H), 4.39(q, 1H), 3.72 (s, 3H), 1.48 (m, 15H)
HOSRSRSSOMe	99%	5.18 (m, 4H), 4.39(q, 1H), 3.72 (s, 3H), 1.48 (m, 15H)
HOSRRRSSOMe	80%	5.18 (m, 4H), 4.39(q, 1H), 3.72 (s, 3H), 1.48 (m, 15H)
HOSSSRSSOMe	81%	5.18 (m, 5H), 4.39(q, 1H), 3.72 (s, 3H), 1.47 (m, 18H)
HORSSRSSOMe	92%	5.18 (m, 5H), 4.39(q, 1H), 3.72 (s, 3H), 1.48 (m, 18H)
HOSRRRSSOMe	79%	5.18 (m, 5H), 4.39(q, 1H), 3.72 (s, 3H), 1.48 (m, 18H)
HORRSRSSOMe	47%	5.18 (m, 5H), 4.39(q, 1H), 3.72 (s, 3H), 1.48 (m, 18H)
HORRSRSSOMe	67%	5.18 (m, 5H), 4.39(q, 1H), 3.72 (s, 3H), 1.48 (m, 18H)
HORRSRSSOMe	67%	5.18 (m, 5H), 4.39(q, 1H), 3.72 (s, 3H), 1.48 (m, 18H)
HOSSSSSSOMe	86%	5.18 (m, 5H), 4.39(q, 1H), 3.72 (s, 3H), 1.48 (m, 18H)
HOSRSSSSOMe	72%	5.18 (m, 5H), 4.39(q, 1H), 3.72 (s, 3H), 1.48 (m, 18H)
HOSRRSSSOMe	80%	5.18 (m, 5H), 4.39(q, 1H), 3.72 (s, 3H), 1.48 (m, 18H)
HORSRSSSOMe	51%	5.18 (m, 5H), 4.39(q, 1H), 3.72 (s, 3H), 1.48 (m, 18H)

Table 3.5. (cont'd).

HORSSSSSOMe	76%	5.18 (m, 5H), 4.39(q, 1H), 3.72 (s, 3H), 1.48 (m, 18H)
HORRSRSSOMe	76%	5.18 (m, 5H), 4.39(q, 1H), 3.72 (s, 3H), 1.48 (m, 18H)
HOSRRSSSOMe	70%	5.18 (m, 5H), 4.39(q, 1H), 3.72 (s, 3H), 1.48 (m, 18H)
HORRRSSSOMe	80%	5.18 (m, 5H), 4.39(q, 1H), 3.72 (s, 3H), 1.48 (m, 18H)
HOSRSRSSOMe	72%	5.18 (m, 5H), 4.39(q, 1H), 3.72 (s, 3H), 1.48 (m, 18H)
HORRSSSSOMe	68%	5.18 (m, 5H), 4.39(q, 1H), 3.72 (s, 3H), 1.48 (m, 18H)
HOSSSRRSOMe	81%	5.18 (m, 5H), 4.39(q, 1H), 3.72 (s, 3H), 1.48 (m, 18H)
HORSSRRSOMe	53%	5.18 (m, 5H), 4.39(q, 1H), 3.72 (s, 3H), 1.48 (m, 18H)
HORRRRRSOMe	62%	5.18 (m, 5H), 4.39(q, 1H), 3.72 (s, 3H), 1.48 (m, 18H)
HOSRRRRSOMe	69%	5.18 (m, 4H), 4.39(q, 1H), 3.72 (s, 3H), 1.48 (m, 18H)
HOSRRSRSOMe	74%	5.18 (m, 5H), 4.39(q, 1H), 3.72 (s, 3H), 1.48 (m, 18H)
HORRRSRSOMe	72%	5.18 (m, 5H), 4.39(q, 1H), 3.72 (s, 3H), 1.48 (m, 18H)
HOSRRSSSOMe	87%	5.18 (m, 5H), 4.39(q, 1H), 3.72 (s, 3H), 1.48 (m, 18H)
HORSSRRSOMe	85%	5.18 (m, 5H), 4.39(q, 1H), 3.72 (s, 3H), 1.48 (m, 18H)
HOSRSRRSOMe	91%	5.18 (m, 5H), 4.39(q, 1H), 3.72 (s, 3H), 1.48 (m, 18H)

Table 3.5. (cont'd).

HORRSRRSOMe	81%	5.18 (m, 5H), 4.39(q, 1H), 3.72 (s, 3H), 1.48 (m, 18H)
HOSSRSRSOMe	63%	5.18 (m, 4H), 4.39(q, 1H), 3.72 (s, 3H), 1.48 (m, 18H)
HORSRSRSOMe	90%	5.18 (m, 5H), 4.39(q, 1H), 3.72 (s, 3H), 1.48 (m, 18H)
HORSSSSSOMe	79%	5.18 (m, 5H), 4.39(q, 1H), 3.72 (s, 3H), 1.48 (m, 18H)
HORSRSSSOMe	30%	5.18 (m, 5H), 4.39(q, 1H), 3.72 (s, 3H), 1.48 (m, 18H)
HORSSSRSOMe	74%	5.18 (m, 5H), 4.39(q, 1H), 3.72 (s, 3H), 1.48 (m, 18H)
HOSSSSRSOMe	57%	5.18 (m, 5H), 4.39(q, 1H), 3.72 (s, 3H), 1.48 (m, 18H)
HORSSRRSOMe	99%	5.18 (m, 5H), 4.39(q, 1H), 3.72 (s, 3H), 1.48 (m, 18H)
HORRRSRSOMe	82%	5.18 (m, 5H), 4.39(q, 1H), 3.72 (s, 3H), 1.48 (m, 18H)
HOSRRSRSOMe	92%	5.18 (m, 5H), 4.39(q, 1H), 3.72 (s, 3H), 1.48 (m, 18H)

Table 3.6. Yields and ^{1}H-NMR Data for Benzyl-terminated Diads

Compound	% Yield	^{1}H NMR (300 MHz, $CDCl_3$)
BnOSSOMe	74%	7.34 (m, 5H), 5.16 (q, 1H), 4.52 (dd, 2H), 3.76 (s, 3H), 1.48 (d, 3H), 1.40 (d, 3H)
BnORSOMe	77%	7.31 (m, 5H), 5.18 (q, 1H), 4.58 (q, 1H), 4.18 (q, 1H), 3.75 (s, 3H), 1.51 (d, 3H), 1.48 (d, 3H)

Table 3.7. Yields and ^{1}H-NMR Data for Benzyl-terminated Triads

Compound	% Yield	^{1}H NMR (300 MHz, $CDCl_3$)
BnORRSOMe	74%	7.31 (m, 5H), 5.18(m, 2H), 4.52 (dd, 2H), 4.13 (q, 1H), 3.72 (s, 3H), 1.56 (d, 3H), 1.49 (d, 3H), 1.42 (d, 3H)
BnORRSOMe	61%	7.31 (m, 5H), 5.18(m, 2H), 4.52 (dd, 2H), 4.13 (q, 1H), 3.72 (s, 3H), 1.56 (d, 3H), 1.49 (d, 3H), 1.42 (d, 3H)
BnOSRSOMe	86%	7.31 (m, 5H), 5.18(m, 2H), 4.52 (dd, 2H), 4.13 (q, 1H), 3.72 (s, 3H), 1.56 (d, 3H), 1.49 (d, 3H), 1.42 (d, 3H)
BnORSSOMe	93%	7.31 (m, 5H), 5.18(m, 2H), 4.52 (dd, 2H), 4.13 (q, 1H), 3.72 (s, 3H), 1.56 (d, 3H), 1.49 (d, 3H), 1.42 (d, 3H)

Table 3.8. Yields and ^{1}H-NMR Data for Benzyl-terminated Tetrads

Compound	% Yield	^{1}H NMR (300 MHz, $CDCl_3$)
BnORRSSOMe	72%	7.28 (m, 5H), 5.15 (m, 5H), 4.59 (dd, 2H), 4.13 (q, 1H), 3.72 (s, 3H), 1.51 (m, 12H)
BnOSRSSOMe	68%	7.28 (m, 5H), 5.15 (m, 5H), 4.59 (dd, 2H), 4.13 (q, 1H), 3.72 (s, 3H), 1.51 (m, 12H)
BnOSRSSOMe	84%	7.28 (m, 5H), 5.15 (m, 5H), 4.59 (dd, 2H), 4.13 (q, 1H), 3.72 (s, 3H), 1.51 (m, 12H)
BnOSRRSOMe	77%	7.28 (m, 5H), 5.15 (m, 5H), 4.59 (dd, 2H), 4.13 (q, 1H), 3.72 (s, 3H), 1.51 (m, 12H)
BnORRRSOMe	64%	7.28 (m, 5H), 5.15 (m, 5H), 4.59 (dd, 2H), 4.13 (q, 1H), 3.72 (s, 3H), 1.51 (m, 12H)
BnORRSSOMe	81%	7.28 (m, 5H), 5.15 (m, 5H), 4.59 (dd, 2H), 4.13 (q, 1H), 3.72 (s, 3H), 1.51 (m, 12H)
BnOSSSSOMe	64%	7.28, (m, 5H), 5.15 (m, 5H), 4.59 (dd, 2H), 4.13 (q, 1H), 3.72 (s, 3H), 1.51 (m, 12H)
BnOSRRSOMe	47%	7.28 (m, 5H), 5.15 (m, 5H), 4.59 (dd, 2H), 4.13 (q, 1H), 3.72 (s, 3H), 1.51 (m, 12H)
BnORSSSOMe	65%	7.28 (m, 5H), 5.15 (m, 5H), 4.59 (dd, 2H), 4.13 (q, 1H), 3.72 (s, 3H), 1.51 (m, 12H)
BnOSSRSOMe	64%	7.38 (m, 5H), 5.17 (m, 3H), 4.57 (dd, 2H), 4.12 (q, 1H), 3.72 (s, 3H), 1.51 (m, 12H)
BnORSRSOMe	64%	7.37 (m, 5H), 5.17 (m, 3H), 4.58 (dd, 2H), 4.17 (q, 1H), 3.71(s, 3H), 1.51 (m, 12H)

Table 3.9. Yields and ^{1}H-NMR Data for Benzyl-terminated Pentads

Compound	% Yield	^{1}H NMR (300 MHz, $CDCl_3$)
BnOSRSRSOMe	92%	7.36 (m, 5H), 5.18 (m, 4H), 4.58 (dd, 2H), 4.10 (q, 1H), 3.72 (s, 3H), 1.50 (m, 15H)
BnOSSSSSOMe	89%	7.36 (m, 5H), 5.18 (m, 4H), 4.58 (dd, 2H), 4.10 (q, 1H), 3.72 (s, 3H), 1.50 (m, 15H)
BnOSRSSSOMe	85%	7.36 (m, 5H), 5.18 (m, 4H), 4.58 (dd, 2H), 4.10 (q, 1H), 3.72 (s, 3H), 1.50 (m, 15H)
BnOSSRSSOMe	97%	7.36 (m, 5H), 5.18 (m, 4H), 4.58 (dd, 2H), 4.10 (q, 1H), 3.72 (s, 3H), 1.50 (m, 15H)
BnORRSRSOMe	73%	7.36 (m, 5H), 5.18 (m, 4H), 4.58 (dd, 2H), 4.10 (q, 1H), 3.72 (s, 3H), 1.50 (m, 15H)
BnORRRSSOMe	90%	7.36 (m, 5H), 5.18 (m, 4H), 4.58 (dd, 2H), 4.10 (q, 1H), 3.72 (s, 3H), 1.50 (m, 15H)
BnOSRRSSOMe	90%	7.36 (m, 5H), 5.18 (m, 4H), 4.58 (dd, 2H), 4.10 (q, 1H), 3.72 (s, 3H), 1.50 (m, 15H)
BnORSRSSOMe	61%	7.36 (m, 5H), 5.18 (m, 4H), 4.58 (dd, 2H), 4.10 (q, 1H), 3.72 (s, 3H), 1.50 (m, 15H)
BnOSRRRSOMe	91%	7.36 (m, 5H), 5.18 (m, 4H), 4.58 (dd, 2H), 4.10 (q, 1H), 3.72 (s, 3H), 1.50 (m, 15H)
BnORRRRSOMe	53%	7.36 (m, 5H), 5.18 (m, 4H), 4.58 (dd, 2H), 4.10 (q, 1H), 3.72 (s, 3H), 1.50 (m, 15H)
BnOSSSSSOMe	79%	7.36 (m, 5H), 5.18 (m, 4H), 4.58 (dd, 2H), 4.10 (q, 1H), 3.72 (s, 3H), 1.50 (m, 15H)
BnOSRSSSOMe	26%	7.36 (m, 5H), 5.18 (m, 4H), 4.58 (dd, 2H), 4.10 (q, 1H), 3.72 (s, 3H), 1.50 (m, 15H)
BnORRSRSOMe	95%	7.28 (m, 5H), 5.17 (m, 4H), 4.58 (dd, 2H), 4.13 (q, 1H) 3.71 (s, 3H), 1.31 (m, 5H)
BnORSSRSOMe	94%	7.36 (m, 5H), 5.18 (m, 4H), 4.58 (dd, 2H), 4.10 (q, 1H), 3.72 (s, 3H), 1.50 (m, 15H)

Table 3.9 (cont'd).

BnOSSSRSOMe	91%	7.31 (m, 5H), 5.13 (m, 4H), 4.60 (dd, 2H), 4.11 (q, 1H), 3.72 (s, 3H), 1.53 (m, 15H)
BnORSRRSOMe	89%	7.31 (m, 5H), 5.17 (m, 4H), 4.57 (dd, 2H), 4.17 (q, 1H), 3.72 (s, 3H), 1.50 (m, 15H)
BnOSSRRSOMe	90%	7.31 (m, 5H), 5.17 (m, 4H), 4.57 (dd, 2H), 4.17 (q, 1H), 3.72 (s, 3H), 1.50 (m, 15H)

Table 3.10. Yields and ^{1}H-NMR Data for Benzyl-terminated Hexads.

Compound	% Yield	^{1}H NMR (300 MHz, $CDCl_3$)
BnORSSRRSOMe	99%	7.28 (m, 5H), 5.15 (m, 5H), 4.59 (dd, 2H), 4.13 (q, 1H), 3.72 (s, 3H), 1.51 (m, 18H)
BnOSRRRSSOMe	99%	7.28 (m, 5H), 5.18 (m, 5H), 4.58 (dd, 2H), 4.12 (q, 1H), 3.72 (s, 3H), 1.52 (m, 18H)
BnORRRRSSOMe	67%	7.28 (m, 5H), 5.18 (m, 5H), 4.58 (dd, 2H), 4.12 (q, 1H), 3.72 (s, 3H), 1.52 (m, 18H)
BnOSSRRSSOMe	76%	7.28 (m, 5H), 5.18 (m, 5H), 4.58 (dd, 2H), 4.12 (q, 1H), 3.72 (s, 3H), 1.52 (m, 18H)
BnORSRRSSOMe	92%	7.28 (m, 5H), 5.18 (m, 5H), 4.58 (dd, 2H), 4.12 (q, 1H), 3.72 (s, 3H), 1.52 (m, 18H)
BnOSRSRSSOMe	87%	7.28 (m, 5H), 5.18 (m, 5H), 4.58 (dd, 2H), 4.12 (q, 1H), 3.72 (s, 3H), 1.52 (m, 18H)
BnORSSRSSOMe	68%	7.28 (m, 5H), 5.18 (m, 5H), 4.58 (dd, 2H), 4.12 (q, 1H), 3.72 (s, 3H), 1.52 (m, 18H)
BnOSSSRSSOMe	47%	7.28 (m, 5H), 5.18 (m, 5H), 4.58 (dd, 2H), 4.12 (q, 1H), 3.72 (s, 3H), 1.52 (m, 18H)
BnORRSRSSOMe	85%	7.28 (m, 5H), 5.18 (m, 5H), 4.58 (dd, 2H), 4.12 (q, 1H), 3.72 (s, 3H), 1.52 (m, 18H)
BnOSRSRSSOMe	98%	7.28 (m, 5H), 5.18 (m, 5H), 4.58 (dd, 2H), 4.12 (q, 1H), 3.72 (s, 3H), 1.52 (m, 18H)
BnOSSSSSSOMe	83%	7.28 (m, 5H), 5.18 (m, 5H), 4.58 (dd, 2H), 4.12 (q, 1H), 3.72 (s, 3H), 1.52 (m, 18H)
BnOSRSSSSOMe	90%	7.28 (m, 5H), 5.18 (m, 5H), 4.58 (dd, 2H), 4.12 (q, 1H), 3.72 (s, 3H), 1.52 (m, 18H)
BnOSSRSSSOMe	43%	7.28 (m, 5H), 5.18 (m, 5H), 4.58 (dd, 2H), 4.12 (q, 1H), 3.72 (s, 3H), 1.52 (m, 18H)
BnOSRRSSSOMe	57%	7.28 (m, 5H), 5.18 (m, 5H), 4.58 (dd, 2H), 4.12 (q, 1H), 3.72 (s, 3H), 1.52 (m, 18H)

Table 3.10. (cont'd).

BnORRRSSSOMe	94%	7.28 (m, 5H), 5.18 (m, 5H), 4.58 (dd, 2H), 4.12 (q, 1H), 3.72 (s, 3H), 1.52 (m, 18H)
BnORSSSSSOMe	65%	7.28 (m, 5H), 5.18 (m, 5H), 4.58 (dd, 2H), 4.12 (q, 1H), 3.72 (s, 3H), 1.52 (m, 18H)
BnORRSSSSOMe	91%	7.28 (m, 5H), 5.18 (m, 5H), 4.58 (dd, 2H), 4.12 (q, 1H), 3.72 (s, 3H), 1.52 (m, 18H)
BnOSRRSSSOMe	98%	7.28 (m, 5H), 5.18 (m, 5H), 4.58 (dd, 2H), 4.12 (q, 1H), 3.72 (s, 3H), 1.52 (m, 18H)
BnOSRSRSSOMe	84%	7.28 (m, 5H), 5.18 (m, 5H), 4.58 (dd, 2H), 4.12 (q, 1H), 3.72 (s, 3H), 1.52 (m, 18H)
BnOSSSRRSOMe	92%	7.28 (m, 5H), 5.18 (m, 5H), 4.58 (dd, 2H), 4.12 (q, 1H), 3.72 (s, 3H), 1.52 (m, 18H)
BnOSRRRRSOMe	69%	7.28 (m, 5H), 5.18 (m, 5H), 4.58 (dd, 2H), 4.12 (q, 1H), 3.72 (s, 3H), 1.52 (m, 18H)
BnORRRRRSOMe	47%	7.28 (m, 5H), 5.18 (m, 5H), 4.58 (dd, 2H), 4.12 (q, 1H), 3.72 (s, 3H), 1.52 (m, 18H)
BnOSSRSRSOMe	30%	7.28 (m, 5H), 5.18 (m, 5H), 4.58 (dd, 2H), 4.12 (q, 1H), 3.72 (s, 3H), 1.52 (m, 18H)
BnORSRSRSOMe	47%	7.28 (m, 5H), 5.18 (m, 5H), 4.58 (dd, 2H), 4.12 (q, 1H), 3.72 (s, 3H), 1.52 (m, 18H)
BnORRSRSSOMe	55%	7.28 (m, 5H), 5.18 (m, 5H), 4.58 (dd, 2H), 4.12 (q, 1H), 3.72 (s, 3H), 1.52 (m, 18H)
BnOSRRSRSOMe	88%	7.28 (m, 5H), 5.18 (m, 5H), 4.58 (dd, 2H), 4.12 (q, 1H), 3.72 (s, 3H), 1.52 (m, 18H)
BnORRRSRSOMe	91%	7.28 (m, 5H), 5.18 (m, 5H), 4.58 (dd, 2H), 4.12 (q, 1H), 3.72 (s, 3H), 1.52 (m, 18H)
BnOSRSRRSOMe	88%	7.28 (m, 5H), 5.18 (m, 5H), 4.58 (dd, 2H), 4.12 (q, 1H), 3.72 (s, 3H), 1.52 (m, 18H
BnORRSRRSOMe	93%	7.28 (m, 5H), 5.18 (m, 5H), 4.58 (dd, 2H), 4.12 (q, 1H), 3.72 (s, 3H), 1.52 (m, 18H)

Table 3.10. (cont'd).

BnOSSSRRSOMe	79%	7.28 (m, 5H), 5.18 (m, 5H), 4.58 (dd, 2H), 4.12 (q, 1H), 3.72 (s, 3H), 1.52 (m, 18H)
BnOSRSSRSOMe	82%	7.28 (m, 5H), 5.18 (m, 5H), 4.58 (dd, 2H), 4.12 (q, 1H), 3.72 (s, 3H), 1.52 (m, 18H
BnORRSSRSOMe	67%	7.28 (m, 5H), 5.18 (m, 5H), 4.58 (dd, 2H), 4.12 (q, 1H), 3.72 (s, 3H), 1.52 (m, 18H)
BnORSSSSSOMe	63%	7.28 (m, 5H), 5.18 (m, 5H), 4.58 (dd, 2H), 4.12 (q, 1H), 3.72 (s, 3H), 1.52 (m, 18H)
BnORSSRRSOMe	71%	7.28 (m, 5H), 5.18 (m, 5H), 4.58 (dd, 2H), 4.12 (q, 1H), 3.72 (s, 3H), 1.52 (m, 18H)
BnOSSSRRSOMe	66%	7.28 (m, 5H), 5.18 (m, 5H), 4.58 (dd, 2H), 4.12 (q, 1H), 3.72 (s, 3H), 1.52 (m, 18H)
BnORRRSRSOMe	98%	7.28 (m, 5H), 5.18 (m, 5H), 4.58 (dd, 2H), 4.12 (q, 1H), 3.72 (s, 3H), 1.52 (m, 18H)
BnOSRRSRSOMe	85%	7.28 (m, 5H), 5.18 (m, 5H), 4.58 (dd, 2H), 4.12 (q, 1H), 3.72 (s, 3H), 1.52 (m, 18H)
BnOSSSSSSOMe	92%	7.28 (m, 5H), 5.18 (m, 5H), 4.58 (dd, 2H), 4.12 (q, 1H), 3.72 (s, 3H), 1.52 (m, 18H)
BnOSSSSRSOMe	87%	7.26 (m, 5H), 5.17 (m, 5H), 4.60 (dd, 2H), 4.18 (q, 1H), 3.71 (s, 3H), 1.51 (m, 21H)
BnORSSSRSOMe	91%	7.28 (m, 5H), 5.18 (m, 5H), 4.58 (dd, 2H), 4.12 (q, 1H), 3.72 (s, 3H), 1.52 (m, 18H)
BnORSRSSSOMe	97%	7.31 (m, 5H), 5.12 (m, 5H), 4.51 (dd, 2H), 4.16 (q, 1H), 3.71 (s, 3H), 1.50 (m, 18H)

Table 3.11. Yield and ^{13}C-NMR Data for (S)-Acetoxypropanoic Acid Methyl Ester

Compound	% Yield	^{13}C NMR (500 MHz, $CDCl_3$)
AcOSOMe	80%	171.18, 170.24, 68.81, 52.48, 20.45, 16.68

Table 3.12. Yields and ^{1}H- and ^{13}C-NMR Data for Acetoxy-terminated Diads.

Compound	% Yield	^{1}H NMR (300 MHz, $CDCl_3$)	^{13}C NMR (500 MHz, $CDCl_3$)
AcOSSOMe	83%	5.10 (m, 2H), 3.70 (s, 3H), 2.10 (s, 3H), 1.51 (d, 3H), 1.48 (d, 3H	170.16, 169.77, 169.72, 68.59, 67.89, 51.81, 19.98, 16.28, 16.21
AcORSOMe	85%	5.10 (m, 2H), 3.70 (s, 3H), 2.10 (s, 3H), 1.51 (d, 3H), 1.48 (d, 3H)	

Table 3.13. Yield and ^{1}H- and ^{13}C-NMR Data for the Acetoxy-terminated Triad.

Compound	% Yield	^{1}H NMR (300 MHz, $CDCl_3$)	^{13}C NMR (500 MHz, $CDCl_3$)
AcORSSOMe	68%	5.17 (m, 3H), 3. 17 (s, 3H), 2.12 (s, 3H), 1.61 (m, 9H)	170.59, 170.16, 170.10, 169.44, 69.18, 68.93, 68.49, 52.23, 20.51, 16.86, 16.76, 16.64

Table 3.14. Yields and ^{1}H- and ^{13}C-NMR Data for Acetoxy-terminated Tetrads

Compound	% Yield	^{1}H NMR (300 MHz, $CDCl_3$)	^{13}C NMR (500 MHz, $CDCl_3$)
AcORSSSOMe	67%	5.17 (m, 4H), 3. 17 (s, 3H), 2.12 (s, 3H), 1.61 (m, 12H)	170.51, 170.11, 170.07, 169.58, 169.43, 69.13, 68.98, 68.84, 68.45, 52.33, 20.53, 16.80, 16.71, 16.61, 16.53
AcOSSSSOMe	65%	5.17 (m, 4H), 3. 17 (s, 3H), 2.12 (s, 3H), 1.61 (m, 15H)	170.54, 170.09, 169.45, 69.14, 69.00, 68.86, 68.47, 52.36, 29.65, 20.55, 16.82, 16.74, 16.64, 16.55

Table 3.15. Yields and ^{1}H- and ^{13}C-NMR Data for Acetoxy-terminated Pentads

Compound	% Yield	^{1}H NMR (300 MHz, $CDCl_3$)	^{13}C NMR (500 MHz, $CDCl_3$)
AcOSRRSSOMe	65%	5.16 (m, 5H), 3.15 (s, 3H), 2.10 (s, 3H), 1.62 (m, 15H)	170.55, 170.09, 169.96, 169.37, 169.31, 169.28, 169.26, 69.39, 69.21, 69.17, 66.05, 68.97, 68.39, 52.38, 20.59, 16.82, 16.75, 16.72, 16.67, 16.62, 16.59
AcOSRSSSOMe	62%	5.16 (m, 5H), 3.15 (s, 3H), 2.10 (s, 3H), 1.62 (m, 15H)	170.43, 169.98, 169.89, 169.49, 169.36, 169.25, 69.19, 69.08, 68.93, 69.91, 68.28, 52.27, 20.47, 16.71, 16.66, 16.65, 16.49, 16.47
AcOSSRSSOMe	95%	5.16 (m, 5H), 3.15 (s, 3H), 2.10 (s, 3H), 1.62 (m, 15H)	170.50, 170.27, 170.03, 169.35, 169.19, 69.31, 69.16, 69.02, 68.86, 68.24, 52.30, 29.61, 20.50, 16.71, 16.68, 16.66, 16.49
AcORSRSSOMe	91%	5.16 (m, 5H), 3.15 (s, 3H), 2.10 (s, 3H), 1.62 (m, 15H)	170.56, 169.39, 169.35, 69.30, 69.23, 69.17, 69.07, 69.05, 68.97, 68.364, 66.70, 52.39, 20.58, 20.06, 16.78, 16.74, 16.61
AcOSRRSSOMe	79%	5.16 (m, 5H), 3.15 (s, 3H), 2.10 (s, 3H), 1.62 (m, 15H)	170.51, 170.10, 170.03, 169.35, 169.29, 169.25, 69.17, 69.10, 69.00, 68.82, 68.45, 52.33, 20.54, 16.81, 16.70, 16.67, 16.64, 16.58
AcOSSSSSOMe	37%	5.16 (m, 5H), 3.15 (s, 3H), 2.10 (s, 3H), 1.62 (m, 15H)	170.30, 170.26, 169.67, 169.55, 169.51, 69.12, 68.97, 68.89, 68.82, 68.26, 52.33, 20.52, 16.70, 16.60, 16.55

Table 3.15 (cont'd).

AcOSRSSSOMe	59%	5.16 (m, 5H), 3.15 (s, 3H), 2.10 (s, 3H), 1.62 (m, 15H)	170.44, 169.99, 169.98, 169.49, 169.38, 169.26, 69.19, 69.08, 68.93, 68.91, 68.28, 52.27, 20.46, 16.70, 16.65, 16.48
AcORRSSSOMe	65%	5.16 (m, 5H), 3.15 (s, 3H), 2.10 (s, 3H), 1.62 (m, 15H)	170.51, 170.28, 170.08, 169.57, 169.47, 169.33, 69.15, 69.02, 68.99, 68.94, 68.24, 52.36, 20.54, 16.73, 16.61, 16.54

Table 3.16. Yields and ^{1}H- and ^{13}C-NMR Data for Acetoxy-terminated Hexads

Compound	% Yield	^{1}H NMR (300 MHz, $CDCl_3$)	^{13}C NMR (500 MHz, $CDCl_3$)
AcOSSSSSSOMe	68%	5.16 (m, 6H), 3.15 (s, 3H), 2.10 (s, 3H), 1.62 (m, 18H)	170.53, 170.37, 170.32, 169.73, 169.56, 69.21, 69.05, 69.00, 68.95, 68.88, 68.33,16.77, 16.66
AcORSSSSSOMe	71%	5.16 (m, 6H), 3.15 (s, 3H), 2.10 (s, 3H), 1.62 (m, 18H)	170.52, 170.14, 170.10, 169.64, 169.60, 169.55, 169.47, 69.20, 69.04, 68.99, 68.88, 68.49, 16.85, 16.76, 16.68, 16.61
AcOSSSSSSOMe	68%	5.16 (m, 6H), 3.15 (s, 3H), 2.10 (s, 3H), 1.62 (m, 18H)	170.53, 170.37, 170.32, 169.73, 169.56, 69.21, 69.05, 69.00, 68.95, 68.88, 68.33,16.77, 16.66
AcORSSSSSOMe	71%	5.16 (m, 6H), 3.15 (s, 3H), 2.10 (s, 3H), 1.62 (m, 18H)	170.52, 170.14, 170.10, 169.64, 169.60, 169.55, 169.47, 69.20, 69.04, 68.99, 68.88, 68.49, 16.85, 16.76, 16.68, 16.61
AcORSRSSSOMe	73%	5.16 (m, 6H), 3.15 (s, 3H), 2.10 (s, 3H), 1.62 (m, 18H)	170.55, 170.07, 169.60, 169.44, 169.33, 69.39, 69.19, 69.04, 69.01, 68.56, 68.39, 16.81, 16.77, 16.72, 16.66, 16.58
AcOSSRRSSOMe	63%	5.16 (m, 6H), 3.15 (s, 3H), 2.10 (s, 3H), 1.62 (m, 18H)	170.55, 170.10, 169.35, 169.17,166.844, 163.69, 163.30, 101.23, 101.08, 69.23, 69.18, 69.07, 69.04, 68.97, 68.28, 21.19, 20.08, 16.74, 16.66, 16.62

Table 3.16. (cont'd)

AcORSSRSSOMe	52%	5.16 (m, 6H), 3.15 (s, 3H), 2.10 (s, 3H), 1.62 (m, 18H)	170.57, 170.18, 170.08, 169.42, 169.32, 169.34, 69.42, 69.23, 69.10, 69.05, 68.89, 68.52, 16.865,16.77, 16.74, 16.69, 16.55
AcOSSSRSSOMe	74%	5.16 (m, 6H), 3.15 (s, 3H), 2.10 (s, 3H), 1.62 (m, 18H)	170.54, 170.35, 170.26, 169.48, 169.29, 169.21, 69.40, 69.20, 69.08, 69.02, 68.84, 68.29, 30.85, 29.66, 20.56, 16.74, 16.71, 16.65, 16.51
AcOSRRRSSOMe	61%	5.16 (m, 6H), 3.15 (s, 3H), 2.10 (s, 3H), 1.62 (m, 18H)	170.57, 170.32, 170.06, 169.41, 169.36, 169.27, 169.15, 69.42, 69.25, 69.22, 69.07, 68.91, 68.29, 16.76, 16.72, 16.71, 16.67, 16.55
AcOSSRSSSOMe	52%	5.16 (m, 6H), 3.15 (s, 3H), 2.10 (s, 3H), 1.62 (m, 18H)	170.55, 170.32, 170.07, 169.58, 169.42, 169.39, 169.25, 69.37, 69.19, 69.04, 68.93, 68.30, 16.77, 16.73, 16.58
AcOSSRRSROMe	63%	5.16 (m, 6H), 3.15 (s, 3H), 2.10 (s, 3H), 1.62 (m, 18H)	170.56, 169.98, 169.38, 169.32, 169.28, 69.39, 69.21, 69.17, 69.05, 68.97, 68.39, 16.81, 16.74, 16.71, 16.65, 16.61, 16.58
AcORRSRSSOMe	68%	5.16 (m, 6H), 3.15 (s, 3H), 2.10 (s, 3H), 1.62 (m, 18H)	170.52, 169.93, 169.38, 169.26, 169.18, 69.35, 69.23, 69.17, 69.13, 69.01, 68.33, 16.70, 16.67, 16.60, 16.58, 16.50

Table 3.16. (cont'd.)

AcOSSRRRSOMe	69%	5.16 (m, 6H), 3.15 (s, 3H), 2.10 (s, 3H), 1.62 (m, 18H)	170.56, 170.32, 170.05, 169.40, 169.35, 169.26, 169.14, 69.39, 69.23, 69.20, 69.04, 68.89, 68.26, 16.75, 16.74, 16.70, 16.68, 16.64, 16.53
AcOSRRSSROMe	71%	5.16 (m, 6H), 3.15 (s, 3H), 2.10 (s, 3H), 1.62 (m, 18H)	170.29, 170.15, 170.02, 169.42, 169.32, 169.25, 169.12, 69.30, 69.14, 69.14, 68.98, 68.85, 68.48, 16.84, 16.77, 16.73, 16.70, 16.66, 16.64
AcOSSSSRSOMe	73%	5.16 (m, 6H), 3.15 (s, 3H), 2.10 (s, 3H), 1.62 (m, 18H)	170.35, 170.30, 170.26, 170.21, 169.43, 169.31, 169.21, 169.08, 69.30, 69.14, 69.14, 68.98, 68.85, 68.48, 16.68, 16.66, 16.63, 16.59, 16.56
AcOSRSSSSOMe	74%	5.16 (m, 6H), 3.15 (s, 3H), 2.10 (s, 3H), 1.62 (m, 18H)	170.23, 170.10, 170.00, 169.58, 169.48, 169.36, 69.29, 69.20, 69.01, 68.39, 16.81, 16.76, 16.61
AcORSRSSSOMe	71%	5.16 (m, 6H), 3.15 (s, 3H), 2.10 (s, 3H), 1.62 (m, 18H)	170.54, 170.08, 169.58, 169.42, 169.32, 169.26, 69.36, 69.17, 69.02, 68.98, 68.36, 16.79, 16.74, 16.70, 16.64, 16.55
AcORSRSSSOMe	71%	5.16 (m, 6H), 3.15 (s, 3H), 2. 10 (s, 3H), 1.62 (m, 18H)	170.54, 170.08, 169.58, 169.42, 169.32, 169.26, 69.36, 69.17, 69.02, 68.98, 68.36, 16.79, 16.74, 16.70, 16.64, 16.55

Table 3.16. (cont'd).

AcORRRRSOMe	68%	5.16 (m, 6H), 3.15 (s, 3H), 2. 10 (s, 3H), 1.62 (m, 18H)	170.52, 170.14, 170.10, 169.64, 169.60, 169.55, 169.47, 69.19, 69.03, 68.98, 68.97, 68.88, 68.49, 20.57, 16.85, 16.76, 16.67, 16.61
AcORRRSRSOMe	65%	5.16 (m, 6H), 3.15 (s, 3H), 2. 10 (s, 3H), 1.62 (m, 18H)	170.54, 170.08, 169.96, 169.59, 169.43, 169.32, 169.26, 69.39, 69.19, 69.19, 69.05, 69.01, 68.39, 16.83, 16.77, 16.73, 16.67, 16.59
AcORRSSRSOMe	52%	5.16 (m, 6H), 3.15 (s, 3H), 2. 10 (s, 3H), 1.62 (m, 18H)	170.55, 170.09, 169.97, 169.38, 169.31, 169.28, 169.26, 69.40, 69.22, 69.17, 69.05, 68.98, 68.40, 16.83, 16.76, 16.67, 16.63, 16.60
AcORRSSSSOMe	72%	5.16 (m, 6H), 3.15 (s, 3H), 2. 10 (s, 3H), 1.62 (m, 18H)	170.52, 170.34, 170.31, 169.66, 169.41, 169.33, 169.29, 69.23, 69.17, 69.08, 69.92, 68.88, 68.32, 16.75, 16.67, 16.63
AcORSRRRSOMe	69%	5.16 (m, 6H), 3.15 (s, 3H), 2. 10 (s, 3H), 1.62 (m, 18H)	170.34, 170.09, 170.05, 169.37, 169.36, 169.24, 169.16, 69.36, 69.28, 69.01, 68.91, 68.82, 68.44, 16.80, 16.51, 16.60, 16.58
AcORSSRRSOMe	82%	5.16 (m, 6H), 3.15 (s, 3H), 2. 10 (s, 3H), 1.62 (m, 18H)	170.31, 170.13, 170.03, 169.43, 169.32, 169.26, 169.13, 69.30, 69.14, 68.98, 68.82, 68.48, 16.84, 16.77, 16.73, 16.70, 16.66, 16.64
AcORRSRRSOMe	68%	5.16 (m, 6H), 3.15 (s, 3H), 2. 10 (s, 3H), 1.62 (m, 18H)	170.54, 170.13, 170.06, 169.40, 169.30, 169.23, 169.22, 69.42, 69.22, 69.10, 69.05, 68.88, 68.51, 16.87, 16.77, 16.74, 16.69, 16.55

Table 3.16. (cont'd).

AcORSRSRSOMe	79%	5.16 (m, 6H), 3.15 (s, 3H), 2.10 (s, 3H), 1.62 (m, 18H)	170.44, 170.09, 169.97, 169.31, 169.23, 169.23, 169.22, 69.39, 69.32, 69.29, 69.28, 69.19, 68.38, 16.84, 16.74, 16.66
AcORSRRSSOMe	43%	5.16 (m, 6H), 3.15 (s, 3H), 2.10 (s, 3H), 1.62 (m, 18H)	170.55, 170.09, 169.96, 169.37, 169.31, 169.28, 169.26, 69.39, 69.21, 69.17, 69.05, 68.97, 68.39, 52.38, 20.59, 16.82, 16.75, 16.72, 16.67, 16.62, 16.59
AcORSSSSSOMe	68%	5.16 (m, 6H), 3.15 (s, 3H), 2.10 (s, 3H), 1.62 (m, 18H)	170.36, 169.96, 169.95, 169.50, 169.45, 169.41, 169.32, 69.08, 68.91, 68.86, 68.85, 68.75, 68.37, 52.25, 20.43, 16.72, 16.55, 16.50, 16.49